TRANSPORTATION RESEARCH RECORD
575

Role of Probability and Statistics in the Structural Analysis of Pavements

5 reports prepared for the 54th Annual Meeting of the Transportation Research Board

TRANSPORTATION
RESEARCH BOARD

NATIONAL RESEARCH
COUNCIL

Washington, D. C., 1976

Transportation Research Record 575
Price $3.20
Edited for TRB by Marjorie Moore

Subject areas
25 pavement design
26 pavement performance
62 foundations (soils)
63 mechanics (earth mass)

Transportation Research Board publications are available by ordering directly from the board. They may also be obtained on a regular basis through organizational or individual supporting membership in the board; members or library subscribers are eligible for substantial discounts. For further information, write to the Transportation Research Board, National Academy of Sciences, 2101 Constitution Avenue, N.W., Washington, D.C. 20418.

The project that is the subject of this report was approved by the Governing Board of the National Research Council, whose members are drawn from the councils of the National Academy of Sciences, the National Academy of Engineering, and the Institute of Medicine. The members of the committee responsible for the report were chosen for their special competence and with regard for appropriate balance.

This report has been reviewed by a group other than the authors according to procedures approved by a Report Review Committee consisting of members of the National Academy of Sciences, the National Academy of Engineering, and the Institute of Medicine.

The views expressed in individual papers and attributed to the authors of those papers are those of the authors and do not necessarily reflect the view of the committee, the Transportation Research Board, the National Academy of Sciences, or the sponsors of the project.

LIBRARY OF CONGRESS CATALOGING IN PUBLICATION DATA

National Research Council. Transportation Research Board.
Role of probability and statistics in the structural analysis of pavements.

(Transportation research record; 575)
1. Pavements–Design and construction–Statistical methods–Addresses, essays, lectures.
I. Title. II. Series.
TE7.H5 no. 575 [TE251] 380.5'08s [625.8] 76-25113
ISBN 0-309-02489-7

CONTENTS

FUNDAMENTALS OF PROBABILITY THEORY

M. E. Harr, Purdue University

The components of a pavement system, its loadings and responses, its constitutive materials, and conditions of weather vary in time and location in a random manner. Mathematical models of such systems are known as stochastic processes. This paper presents some fundamentals of probability theory that form the building blocks of such processes. Specific topics treated are deterministic and stochastic systems, randomness and probability, tree diagrams, permutations and computations, conditional probabilities, independence, and Bayes' theorem. Examples are presented to demonstrate the use of the concepts relative to factors entering the analysis, design, construction, and proofing of pavement systems. The concept of chance as it applies to dice or cards is discussed. In this paper a collection of tools is described, and their use is demonstrated.

•ACHIEVEMENTS in transportation technology during the last 2 decades have increased the need for pavement evaluation procedures with which to assess the future trends of pavement behavior. The rates and magnitudes of loadings imposed on today's pavement systems surpass those previously experienced, especially those due to air transport vehicles. The nature of these loadings places greater demands on pavements than they were designed and constructed for. The deterioration of today's pavements has become a major problem of civil engineering.

The problem facing the profession today is not how to design and build new pavement systems for greater frequency and magnitude of loadings, but how to upgrade and provide the remedial measures for existing pavement systems to meet current and future traffic demands.

In pavement design and analysis, factors that are commonly swept under the carpet in other analytical problem areas cannot be assumed away. For example, a pavement consists of distinct layers with unknown contacts at their interface; the layers may or may not be in contact in space or in time. Imposed loadings (wheels) are relatively large in area compared with the thickness of the surface layer; consequently, Saint-Venant's principle cannot be invoked to change the system to an equivalent homogeneous and isotropic body. Ambient conditions greatly alter the properties of the layers, which range from thermal plastic, temperature-sensitive materials to granular soils whose actions depend greatly on their voids. Each layer is composed of complex conglomerations of discrete particles of varying shapes, sizes, and orientations. In addition, loads are variable in both magnitude and time and are dynamic in nature. It is not surprising how poor predictions of the transmission of induced energy through such systems have been. Randomness alone dictates the probabilistic (casual) rather than deterministic (causal) treatment.

DETERMINISTIC AND STOCHASTIC SYSTEMS

Systems that can be described by unique explicit mathematical relationships are said to be deterministic. An example of a common deterministic system is shown in Figure 1a. The system is composed of the mass m, suspended from a linear spring (with spring constant k), which is displaced an amount Δ from its equilibrium position. The mathematical relationship of the response y(t) is

$$y(t) = \Delta \cos \sqrt{\frac{k}{m}}\, t \qquad (1)$$

for $t \geq 0$. This expression provides the unique position of the mass y(t) at any instant of time; hence, the system is completely determined or deterministic. A pictorial representation of the model is shown in Figure 1b. An example of the use of this model with respect to pavements was given by Harr (3).

The concept of a stochastic system is shown in Figure 2, which illustrates a vertical cross section through a pavement subjected at its surface (the x-axis) to a unit force (say per unit length normal to the plane of the paper) acting at point $x = x_1$. Suppose that we wish to determine the magnitudes of the two forces F_A and F_B, located as shown at equal distances a on either side of the unit force at a constant depth $z = z_1$. In effect, we would seek the transmission of the unit force through the pavement. A pavement, in its general form, is composed of a complex conglomeration of discrete particles, in arrays of varying shapes, sizes, and orientations, and contains randomly distributed concentrations of cementing agents. Certainly, we cannot expect that, in general, the forces registered by F_A and F_B will always be equal. (In the deterministic approach, it is customary to plead symmetry and hence the equality of the two forces, i.e., $F_A = F_B$.) In fact, because of the variations in the characteristics of such media, we should expect that they will seldom be equal because the location $x = x_1$ varies. For example, if one of the forces was not in contact with a solid particle, i.e., was in a void, no force would be noted. Evidently, as the unit force is moved in time, as for moving vehicles, through a series of points $x = x_1$, the magnitudes of the forces would be expected to be random in character, i.e., casual rather than causal. Systems that display random results with time are said to be stochastic. The thesis here is that, to be meaningful, experiments involving such systems should be formulated in terms of probabilistic statements rather than explicit expressions.

RANDOMNESS AND PROBABILITY

As noted, in the deterministic approach the outcomes of experiments (observations or phenomena) are treated as absolute quantities. For example, when given the total weight W, total volume V, and weights of solids W_s for a water-saturated soil mass, the porosity can be obtained from the formula $n = (W - W_s)/V\gamma_w$. In particular, given $W = 100$ g, $W_s = 55$ g, $V = 100$ cm^3, the porosity is n = 45 percent. Implied in this result is that, if we were to carry out the weighings and volumetric determinations on a large number of samples of the soil, under certain similar conditions, we would expect on the average that the ratio of volume of voids to total volume would be 0.45. Obviously, the determined porosity would not be 45 percent in every experiment. Sometimes it would be 40 or 41 percent, other times 43 or 46 percent. Occasionally, it may even be very much smaller or very much greater than 45 percent.

This example illustrates what is meant by random experiments, experiments that can give varying outcomes (results) depending on chance circumstances that are either unknown or beyond control. The distributions of particle sizes in a number of soil samples from the same test pit will not be the same. The variation in measured pavement thickness for a given section will show considerable differences. Contrary to common belief, the inability to obtain concise descriptions of events or observations is not a declaration of ignorance; it is the way nature and the real world behave—fraught with uncertainty. Stated more succinctly, there is no absolute knowledge. What physicists considered exact and ordered prior to the development of quantum mechanics turned out to be merely the mean value of a much more impressive structure.

The diversity of results of apparently similar circumstances is the consequence of randomness. A single data set represents only one of many possible results that may occur. Each of these may be considered as a single result of a random experiment (or phenomenon), the collection of which produces a random process. In other words, a data record for a particular sample of a random phenomenon is only one physical realization of a random process.

Every test and measurement conducted on pavement systems introduces a magnitude whose numerical value depends on random factors that are beyond control. Furthermore, each such magnitude can have a different value in successive trials. This type of magnitude is called a random variable; the separate magnitudes are called elementary events. The outcomes of a random experiment are called elementary events if (a) only one outcome can occur at a time and (b) one outcome always does occur. Condition a specifies that the outcomes are mutually exclusive or are disjoint; that is, no two elementary events can occur simultaneously. Condition b states that an elementary event is possible. The classic example of an elementary event is the outcome of the toss of a fair die. (Historically, questions relative to dice, asked of Pascal, precipitated the mathematical theory of probability.) Condition a is satisfied because only one face can appear per toss of a die. Condition b is ensured because any one of the six faces is likely to appear.

Implied in the die toss experiment is that the numbers 1, 2, 3, 4, 5, and 6 each have a possibility of occurring with equal likelihood. However, the number that will appear on any one toss is uncertain. Suppose now that the experiment is repeated many times. Even though the numbers shown on the faces may be different in successive tosses, it is reasonable to expect that, over the long run, any one number will occur one-sixth of the time. A gambler would say that the odds against tossing any specified number is five to one. The probabilist would define that probability to be one-sixth.

The measure of the probability of an outcome is its relative frequency. That is, if an outcome E can occur n times in N equally likely trials, the probability of the occurrence of outcome E (after a large, theoretically infinitely large, number of experiments) is

$$P(E) = \frac{n}{N} \tag{2}$$

Also, implied in equation 2 is the concept of the ratio of favorable outcome to the number of all possible cases. This definition was first formulated by Laplace in 1812. Stated another way, the probability of outcome A equals the number of outcomes favorable to A divided by the total number of outcomes or

$$P(A) = \frac{\text{favorable outcomes}}{\text{total outcomes}} \tag{3}$$

As an example, find the probability of drawing a red card from an ordinary well-shuffled deck of 52 cards. Of the 52 mutually exclusive and equally likely outcomes (each card is a possible outcome and, hence, an elementary event), there are 26 favorable outcomes (red cards); hence,

$$P(\text{drawing a red card}) = \frac{\text{favorable outcomes}}{\text{total outcomes}} = \frac{26}{52} = \frac{1}{2}$$

Knowledge of the distribution of a random variable and of the probabilities of the various possible values enables predictions to be made of the occurrence of an event or collection of events. The underlying question is, How does one find this distribution? Considering the uses to which probability theory has been put and the length of time it has been around, it is not surprising that there are many avenues available. At this point in our development, it will suffice to list a few examples.

1. Some few experiments are performed, and frequencies are noted and then generalized; e.g., a fair coin will show heads half of the time, or the porosity of the soil layer is 42 percent.
2. Probabilities are assigned subjectively as a set of weights that express likelihoods of outcomes; e.g., each of the 10 questions in the examination is worth 10 points, and 70 is the minimum passing grade.
3. Whole families of distribution laws stem from mathematical excursion derived from certain intuitive concepts. Detailed examples are available in texts dealing with probability (2).

Whatever the basis for assigning probabilities to elementary events or outcomes, the following are axiomatic: The probability of an outcome A ranges between zero and unity

$$0 \leq P(A) \leq 1 \tag{4}$$

and the certainty of an outcome C has a probability of unity

$$P(C) = 1 \tag{5}$$

The probability of the occurrence of a number of elementary events or outcomes A_1, $A_2, \ldots, A_i$ is the sum of component probabilities (addition rule):

$$P(A_1 + A_2 + \ldots + A_i) = P(A_1) + P(A_2) + \ldots + P(A_i) = \sum_{n=1}^{n=i} P(A_n) \tag{6}$$

This also implies that

$$P(A_1 \text{ or } A_2 \text{ or } \ldots A_i) = P(A_1) + P(A_2) + \ldots + P(A_i) \tag{7}$$

Equations 4, 5, 6, and 7 are the building blocks from which the elementary theory of probability is constructed. These axioms will next be used to derive some important properties of the probabilities of mutually exclusive outcomes.

A collection of elementary outcomes, $A_1, A_2, \ldots, A_n$, is said to be collectively exhaustive if it represents all outcomes that can occur for a given experiment. Symbolically, this is shown as

$$S = \{A_1, A_2, \ldots, A_n\} \tag{8}$$

For the toss of a die the six outcomes—$A_1 = 1$ appears, $A_2 = 2$ appears, ..., $A_6 = 6$ appears—are both mutually exclusive and collectively exhaustive; therefore,

$$S = \{A_1, A_2, \ldots, A_6\} \tag{9}$$

From equations 5 and 6 it follows that the probability of a collectively exhaustive set of outcomes is unity:

$$P(S) = P(A_1) + P(A_2) + \ldots + P(A_n) = 1 \tag{10}$$

An event A^c is said to be the complement of outcome A if $A^c + A = 1$. Here $S = \{A, A^c\}$. From equation 10 it follows that

$$P(A^c) = 1 - P(A) \tag{11}$$

It follows from equations 5 and 11 that, if C is the certain outcome, its complement is the uncertain outcome U whose probability is

$$P(U) = 0 \tag{12}$$

As another example, let w represent the square opening of a particular sieve of wire diameter D, and find the probability that a spherical particle of diameter d will hit the wire if the particle falls perpendicular to the plane of the sieve (Figure 3).

The possible outcomes can be related to the location of the center of the sphere relative to the mesh. It will only be necessary to consider one square because all squares present similar situations. The probability of the sphere hitting the mesh can be measured by the likelihood (favorable outcome) of the center of the sphere hitting beyond the dotted square ABCE in Figure 3. The total outcome is measured by the area of the square abce = $(w + D)^2$. Thus, the favorable outcome is the area between square ABCE and square abce = $(w + D)^2 - (w - D - d)^2$. Hence, the probabilities are

$$P(\text{hitting mesh}) = 1 - \left(\frac{w - D - d}{w + D}\right)^2 \tag{12a}$$

and

$$P(\text{passing through opening}) = \left(\frac{w - D - d}{w + D}\right)^2 \tag{12b}$$

This example provides some interesting excursions into what happens during the sieving process. If we assume that there is no interference between particles and that for a No. 200 sieve w = 0.074 mm and D = 0.0021 mm, a particle with a diameter 90 percent of the opening d = 0.067 mm has a probability of 0.9959 of hitting the mesh under the stated conditions. Suppose now that the sieve is shaken through n cycles. If we assume each cycle is equivalent to repeating the sphere dropping process, the probability of the particle hitting the mesh after n cycles is $(0.9959)^n$. To achieve a probability of 90 percent that the particle will pass through the opening—a probability of 0.10 that it will hit the mesh—will require $(0.9959)^n = 0.10$ or n = 554 cycles, hardly a manual task!

Now consider the cross section through a sample of a particulate medium at elevation z (Figure 4). The shaded portion defines the intersection of the plane of the cross section with the solid particles; the unshaded portion represents the region of voids. If m(z) is the area porosity, the ratio of the area of voids $A_v(z)$ (shown unshaded) to the total area A of the section at any elevation z, then

$$m(z) = \frac{A_v(z)}{A}$$

The average value of m(z) over the height of the sample h is

$$m = \frac{1}{h}\int_0^h m(z)dz$$

Then

$$m = \frac{1}{Ah}\int_0^h Am(z)dz = \frac{1}{V}\int_0^h A_v(z)dz$$

where V is the total volume and the integral is the volume of voids. Hence, the average value of m is the volume porosity n. Based on the geometric definition of probability, it follows that the porosity of a particulate material $n = V_v/V$ is the probability of finding (hitting) a void in a unit volume. The complementary event to the porosity is the volume of solids per unit volume $n_s = 1 - n$; therefore, the probability of locating a solid particle in a unit volume of material is

$$P(\text{locating a particle}) = n_s = 1 - n \tag{13}$$

In the limit, when there are no voids, equation 13 shows that the certainty of locating a solid is $n_s = 1$.

TREE DIAGRAMS

The characterization of a sample of a highway pavement requires a choice of one of three identification tests (I_1, I_2, I_3), a choice of one of three strength tests (S_1, S_2, S_3), and a choice of one of two compressibility tests (C_1, C_2). In how many possible ways may the characterization of tests be performed? The three-step process is shown in Figure 5. It should be evident why this representation is called a tree diagram. The total number of outcomes is the same as number of possible paths, which in this case is simply the sum of the twigs on the lowest branch, i.e., the number of C's, which is 18. The ordering of the tests is arbitrary.

As another example, consider that there are four classifications of soils (gravel, sand, silt, and clay), the soils may be saturated or unsaturated, and they may exhibit low, medium, and high degrees of density. If all sequences are equally likely, how probable is it that a randomly selected sample will be a dense, saturated clay?

The tree diagram is shown in Figure 6. There are 24 possibilities; hence the probability of selecting a sample of dense, saturated clay (shown darker) is 1/24.

It should be apparent that the tree diagram is in a sense a graphical multiplier. The same results could have been obtained by using a multiplication rule. Stated simply, if the first step (or event) A_1 has a_1 outcomes and for each of these a_1 outcomes a second independent step (or event) A_2 has a_2 outcomes, then there will be the product a_1a_2 outcomes after the two steps. Obviously, this can be extended to any number of independent events. For the example in Figure 5, this would lead to $3 \times 3 \times 2 = 18$ outcomes. For Figure 6, $4 \times 2 \times 3 = 24$ outcomes.

PERMUTATIONS AND COMBINATIONS

The listing of all the distinct arrangements of r objects within a collection of n objects is called the permutations of n objects taken r at a time. Symbolically, this is shown as

$$P(n, r) = \frac{n!}{(n - r)!} \qquad (14)$$

where $n! = n(n - 1)(n - 2) \ldots (2)(1)$. Other common designations are ${}_nP_r$, P_r^n, and $P_{n,r}$.

Arranging n objects in some order of r is the same as preparing a tree diagram with n ways shown in the first step, n - 1 ways in the second, until n - r + 1 ways occupy the last (the r th) position.

If there are 10 automobiles that at various times occupy the six available parking spaces reserved for employees at the rear of a store, how many different parking arrangements are possible assuming that no parking spaces remain unoccupied?

The question asks, How many groups of six can be arranged from among 10 objects? Thus, n = 10, r = 6, and $P(10, 6) = 10 \times 9 \times 8 \times 7 \times 6 \times 5 = 151{,}200$.

Another common situation is when one wishes to find the number of distinct permutations (remembering that all permutations must be different) when some of the objects in the collection are alike. Suppose that of the n objects n_1 are all of one kind, n_2 are all of a second kind, etc., and there are k kinds. It can be shown that the number of distinct permutations is

$$\frac{n!}{(n_1!\, n_2! \ldots n_k!)} \qquad (15)$$

In how many ways can 15 objects be divided into two groups such that one has twice as many as the other? Here n = 15, $n_1 = 10$, and $n_2 = 5$. Hence applying equation 15 gives $15!/(10! \cdot 5!) = 3{,}003$ ways.

A combination of objects rather than a permutation occurs when order is of no importance. Generally, a combination can be thought of as a selection and a permutation as an arrangement. A combination of n objects taken r at a time is a selection of r objects taken from among the n objects without specifying order or arrangement. For example, the combination of the four letters a, b, c, and d taken three at a time is abc, abd, acd, and bcd. Because order is not important, the combinations abc, acb, cab, cba, bac, and bca are all equal. The number of combinations of r objects from among n objects is given as

$$C(n, r) = \frac{n!}{r!(n - r)!} \qquad (16)$$

This sequence follows from the observation that there are r! permutations of every combination of $P(n, r) = r!\,C(n, r)$. It follows from equation 16 that $C(n, r) = C(n, n - r)$. Other designations are ${}_nC_r$, $C_{n,r}$, C_r^n. Another commonly used symbol for the r combinations of n objects is

$$C(n, r) = \binom{n}{r} \qquad (17)$$

An inspector on a highway project discovers that k of every n samples tested can be expected to be below standard. If n samples are chosen randomly, from a batch of n samples find the probability that ℓ are below standard.

There are a total of $\binom{n}{m}$ number of ways to choose m items out of n. The number of favorable ways is $\binom{k}{\ell} \times \binom{n-k}{m-\ell}$; that is, the favorable outcomes (for this example, not for the inspector) are those in which ℓ substandard tests are found among k items, which can be done $\binom{k}{\ell}$ ways, and the remaining m - ℓ tests are at or above standard from among the total number of n - k tests. Hence the required probability will be the number of favorable ways divided by the total number of ways or

$$P = \frac{\binom{k}{\ell} \times \binom{n-k}{m-\ell}}{\binom{n}{m}} \tag{18}$$

CONDITIONAL PROBABILITIES

Concrete for a particular highway pavement is mixed in two plants P_1 and P_2 and trucked to the jobsite. Plant P_1 produces 66 percent and plant P_2 34 percent of the concrete used. Tests on concrete cylinders judge the concrete to meet standards if the 28-day unconfined compressive strength is no less than 4,500 psi (31 000 kPa). Previous tests on the concrete from plant P_1 show that an average of 91 percent of the concrete meets standards. Results from plant P_2 show that 83 percent of the samples meet the criterion. These results would indicate that the highway inspector can expect, on the average, that approximately 88 tests per 100 will prove adequate $[(0.66) \times (91) + (0.34) \times (83) \approx 88]$. Stated another way, the probability of a sample of concrete meeting the specification is approximately 0.88. If all the concrete was obtained from plant P_1, the probability of getting standard concrete would be 91 percent; plant P_2 would produce 83 percent. It is apparent that information on where the concrete was produced will affect the probability of the outcome. Such probabilities are said to be conditional; that is, the occurrence of one outcome (information on which plant produced the concrete) will modify the chance of the occurrence of another outcome (the probability that a number of test samples of the concrete will test above standard). Before the origin of the concrete was specified, the unconditional probability that the tests would pass the specification was 0.88.

The conditional probability of an outcome A, given that an outcome B has occurred, denoted $P(A|B)$, is defined as

$$P(A|B) = \frac{P(AB)}{P(B)} \tag{19}$$

where P(AB) denotes the probability that both (simultaneous occurrences) outcomes A and B will occur, called their intersection, and P(B) is the probability of the occurrence of outcome B. (In set theory AB, designated $A \cap B$, is the intersection of A and B or the joint occurrence of A and B.) If $P(B) = 0$, the conditional probability is not defined. Other useful forms of this expression are

$$P(AB) = P(A)\,P(B|A)$$

or

$$P(AB) = P(B)\,P(A\,|\,B) \tag{20}$$

These forms yield the probability of the intersection (or simultaneous occurrences) of both outcomes A and B. In words, the simultaneous occurrence of two outcomes is equal to the product of the probability of one outcome and the conditional probability of the other, assuming the first occurred.

For example, a pair of fair dice are thrown. What is the (conditional) probability that their sum is greater than 6 if a 2 appears on the first die?

There are $6^2 = 36$ possible outcomes. The number 2 appearing on the first die has a probability of occurrence of $1/6$. There are two (simultaneous) favorable outcomes: a five or six on the second die. This is the outcome AB. Hence, $P(AB) = 2/36$. Using equation 19 gives a conditional probability of

$$P(A\,|\,B) = \frac{2/36}{1/6} = 2/6 = 1/3$$

An example of the unconditional probability for this example would correspond to asking, What is the probability that a sum greater than 6 will appear on the throw of a pair of dice? Because there are 21 favorable outcomes, the unconditional probability would equal $21/36 = 0.58$.

For a number of problems a tree diagram is very useful in understanding the outcomes and their probabilities.

A box contains 10 articles; six are painted red and four are white. If two articles are selected at random (without replacement), what are the probabilities of the various permutations?

The results are shown on the tree diagram in Figure 7. The probability of any permutation (path) is the product of the branch probabilities. On the first draw, the probability of drawing red is $P(R) = 6/10$. However, on the second draw, because there are only 5 reds available among the 9 articles, $P(R\,|\,R) = 5/9$. Hence from $P(RR) = P(R) \times P(R\,|\,R) = 1/3$. Note that the probability of drawing one of each color at the end of the drawing is $P(RW) + P(WR) = 4/15 + 4/15 = 8/15$.

Equation 20 gives the probability of the joint occurrence (intersection) of two outcomes A and B. These can be further generalized to any number of outcomes. For three outcomes, ABC,

$$P(ABC) = P(A) \times P(B\,|\,A) \times P(C\,|\,AB) \tag{21}$$

where $P(C\,|\,AB)$ is the probability that outcome C occurs given that the joint outcomes of A and B have already occurred.

Find the probability of drawing hearts on three consecutive draws, without replacement, from a standard deck of cards. We define A, B, C as outcomes of a heart being drawn on the first, second, and third draws. Here as in the previous example $P(A) = 1/4$, $P(B\,|\,A) = 4/17$, and $P(C\,|\,AB) = 11/50$. Hence,

$$P(\text{drawing three consecutive hearts}) = 1/4 \times 4/17 \times 11/50 = 0.013$$

Equation 21 can be extended to any number of outcomes. For any outcomes $A_1, A_2, \ldots, A_n$,

$$P(A_1A_2 \ldots A_n) = P(A_1)P(A_2|A_1)P(A_3|A_1A_2) \ldots P(A_n|A_1A_2 \ldots A_{n-1})$$

or

$$P\left(\prod_{k=1}^{n} A_k\right) = P(A_1)P(A_2|A_1)P(A_3|A_1A_2) \ldots P\left(A_n \middle| \prod_{k=1}^{n-1} A_k\right) \tag{22}$$

Equation 22 is called the multiplication rule of probability; the addition rule was given in equation 6.

A sample of gravel from a gravel pit is to be examined to determine whether the pit can furnish adequate coarse aggregate for making concrete. Specifications require that the pit be rejected if at least one deleterious particle is discovered among five particles selected at random from the sample. What is the probability that the gravel pit will be acceptable if a sample of 100 particles contains 5 deleterious particles?

Let A_i be finding a nondeleterious particle as the i th outcome. The probability of acceptance is the probability of the joint outcome $P(A_1A_2A_3A_4A_5)$. The probability of not finding the first deleterious particle is $P(A_1) = 95/100$ because, of the 100 particles, 95 are acceptable. After the occurrence of event A_1, there remain 99 particles of which 94 are not deleterious; hence, $P(A_2|A_1) = 94/99$. Continuing the reasoning, $P(A_3|A_1A_2) = 93/98$, $P(A_4|A_1A_2A_3) = 92/97$, and $P(A_5|A_1A_2A_3A_4) = 91/96$. Therefore, from equation 22,

$$P(\text{acceptance}) = 95/100 \times 94/99 \times 93/98 \times 92/97 \times 91/96 = 0.77$$

The same result can be obtained another way. There are $\binom{95}{5}$ favorable ways that 5 good particles can be selected from among 95 good ones. There are a total of $\binom{100}{5}$ ways of selecting 5 particles from among 100. Hence,

$$P(\text{acceptance}) = \binom{95}{5} \Big/ \binom{100}{5} = 0.77$$

A useful graphical representation of various operations involving outcomes is the Venn diagram. The outcomes are usually represented by simple geometrical shapes. Suppose now that the rectangular region S shown in Figure 8 represents the total probability $P(S) = 1$. Then the probabilities associated with any outcomes are the sum of the elementary outcomes that are contained within their respective regions in the Venn diagram. For example, suppose the dots shown in the figure represent elementary outcomes; those belonging to A are within circle A and those for B within the circle. Where the two circles overlap (shown shaded), some elementary outcomes in A are also in B. This corresponds to the intersection of A and B, which is designated AB or $A \cap B$. The probability that A or B or P(A or B) (of the union of A and B, $A \cup B$) will occur is the sum of the probabilities of their respective elementary outcomes with each elementary outcome accounted for only once. Because the regions overlap, the simple sum of their elementary outcomes $P(A) + P(B)$ would add the elements in the common region twice; hence, in general,

$$P(A \text{ or } B) = P(A) + P(B) - P(AB) \tag{23a}$$

or in set notation

$$P(A \cup B) = P(A) + P(B) - P(A \cap B) \qquad (23b)$$

For the example with the concrete plant mentioned previously, the following outcomes are defined:

A = concrete meets standard,
A^c = concrete does not meet standard,
B = concrete produced at first plant, and
B^c = concrete produced at second plant.

It is immediately apparent that there are no outcomes simultaneously favorable to $P(AA^c)$ and $P(BB^c)$. Such outcomes are mutually exclusive or incompatible; both cannot happen simultaneously. On the other hand, some concrete produced at both plants did not meet standards; hence,

$$P(A) = P(AB) + P(AB^c) \qquad (24a)$$

$$P(B) = P(AB) + P(A^cB) \qquad (24b)$$

What is the probability of the outcomes A or B or both or P(A or B) = ? In other words, what is the probability that the concrete meets the standard or is produced at the first plant or that both conditions are satisfied? From equation 6, it follows that

$$P(A \text{ or } B) = P(AB) + P(AB^c) + P(A^cB)$$

All other possibilities are incompatible. Combining equations 24a and 24b gives the same result as in equation 23.

Of a sample of 100 particles inspected, 15 are deleterious, 8 are too large for the intended use, and 6 have both defects. If a particle is selected at random from the sample, what is the probability that it will not be suitable?

$$P(\text{not suitable}) = P(\text{deleterious}) + P(\text{too large}) - P(\text{both})$$

$$= {}^{15}/_{100} + {}^{8}/_{100} - {}^{6}/_{100} = 0.17$$

Equation 23 demonstrates that, if $P(AB) = 0$, the probability of the joint occurrence is zero and equation 6 applies. The outcomes are said to be independent. Stated another way, two outcomes are independent if the occurrence or nonoccurrence of one has no effect on the probability of the occurrence of the other. Independence implies unconditional probability or $P(A|B) = P(A)$. Hence, for the case of the independence of outcomes, the addition rule is

$$P(A_1 + A_2 + A_3 + \ldots + A_i) = P(A_1) + P(A_2) + \ldots + P(A_i) \qquad (25)$$

and the multiplication rule is

$$P(A_1A_2A_3 \ldots A_i) = P(A_1) \times P(A_2) \times \ldots \times P(A_i) \qquad (26)$$

Find the probability of drawing a heart on three consecutive draws from a standard deck if the cards are replaced and the deck is reshuffled after each draw. As stated, each draw is independent of the other; hence, the probability of drawing a heart each time is $\frac{1}{4}$, and

$$P(\text{drawing three consecutive hearts}) = \tfrac{1}{4} \times \tfrac{1}{4} \times \tfrac{1}{4} = 0.016$$

Without replacement, the probability is slightly less, 0.013.

The scheme shown in Figure 9 represents the road system between two cities. R_M and R_N are city roads, and S_1, S_2, and S_3 are state highways. After a major snowstorm the probabilities of the various highways being impassable are as shown in the figure. What is the probability of a driver being able to get from city M to city N under the stated conditions if his or her choice of state highway is random?

The probability of the system being open is the complement of it being closed. If p is the probability of impassability,

$$p = P(R \text{ or } S) = P(R) + P(S) - P(RS)$$

where R and S are the outcomes that a city highway or a state highway is impassable. Hence, $P(R) = P(R_M) + P(R_N) - P(R_M)\,P(R_N)$ because outcomes R_M and R_N are independent. That is, $P(R_MR_N) = P(R_M) \times P(R_N|R_M) = P(R_M) \times P(R_N)$. Thus, $P(R) = 0.6 + 0.5 - (0.6) \times (0.5) = 0.8$. $P(S) = P(S_1)\,P(S_2)\,P(S_3)$ because each state highway is independent of the other. Thus $P(S) = (0.4)(0.7)(0.9) = 0.252$. Furthermore, because R and S are independent, $P(RS) = P(R) \times P(S) = (0.8)(0.252) = 0.202$. Therefore, $p = 0.800 + 0.252 - 0.202 = 0.85$ and $P(\text{driving between the cities}) = 1 - 0.85 = 0.15$.

BAYES' THEOREM

Suppose that n outcomes $A_1A_2A_3, \ldots, A_n$ are mutually exclusive and collectively exhaustive such that $\sum_{i=1}^{n} P(A_i) = 1$. Suppose also that there is another outcome B whose occurrence was preceded by or caused by one of the n outcomes of A_i; which of the outcomes in A_i is not known. Because an outcome in A_i precipitated B, it is said to be prior or an a priori outcome. The occurrence of outcome B (called an a posteriori outcome) requires the occurrence of one of the joint outcomes A_iB, which, in general, can be written as

$$P(B) = \sum_{i=1}^{n} P(A_iB)$$

Using the multiplication rule gives

$$P(B) = P(B\,|\,A_1) \times P(A_1) + P(B\,|A_2) \times P(A_2) + \ldots + P(B\,|\,A_n) \times P(A_n)$$

$$= \sum_{i=1}^{n} P(B\,|\,A_i)P(A_i) \tag{27}$$

Equation 27 is called the total probability theorem.

A boring record at the site of a bridge abutment for an overpass indicates that 30 percent of the soil profile of interest is sand, 25 percent silty-sand, 25 percent silty clay, and 20 percent clay. Samples are taken at the site in proportion to layer thickness; however, for various reasons, not all the samples are reliable. Indications are that only 27 percent of the sand samples are adequate, 10 percent of the silty-sand, 30 percent of the silty clay, and 50 percent of the clay. If we wish to examine in detail the soil characteristics at a particular depth, what is the probability that one of the samples chosen at random will furnish reliable information?

Designate the initial samples as A_s, A_{ss}, A_{sc}, and A_c. The prior probabilities were $P(A_s) = 0.3$, $P(A_{ss}) = 0.25$, $P(A_{sc}) = 0.25$, $P(A_c) = 0.20$. If B denotes that the sample at the desired depth is among the reliable samples, the probable occurrences are $P(B\,|\,A_s) = 0.27$, $P(B\,|\,A_{ss}) = 0.10$, $P(B\,|\,A_{sc}) = 0.30$, $P(B\,|\,A_c) = 0.50$. Hence, the required probability is

$$P(B) = (0.3)(0.27) + (0.25)(0.10) + (0.25)(0.30) + (0.20)(0.50) = 0.28$$

Again assume that the prior outcomes A_1, $A_2, \ldots, A_n$ are mutually exclusive and collectively exhaustive. Also suppose that the outcome of B is preceded by or caused by one of the A_i. Again, which one is not known. From equation 20,

$$P(A_iB) = P(A_i) \times P(B\,|\,A_i)$$

or

$$P(A_iB) = P(B) \times P(B\,|\,A_i)$$

from which

$$P(A_i\,|\,B) = \frac{P(A_i)\,P(B\,|\,A_i)}{P(B)} \tag{28}$$

Expressing P(B) by using the total probability equation (equation 27) produces

$$P(A_i\,|\,B) = \frac{P(A_i) \times P(B\,|\,A_i)}{\sum_{i=1}^{n} P(B\,|\,A_i) \times P(A_i)} \tag{29}$$

This result is called Bayes' theorem. It indicates how opinions held before an experiment should be modified by the evidence of the outcome. Historically, its statement

Figure 1. (a) Deterministic system and (b) model.

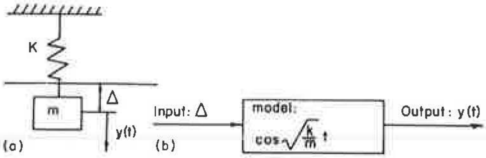

Figure 2. Example of stochastic system.

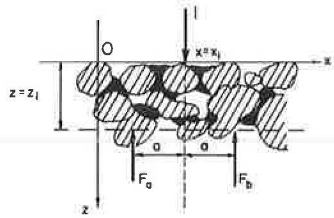

Figure 3. Sieve opening example.

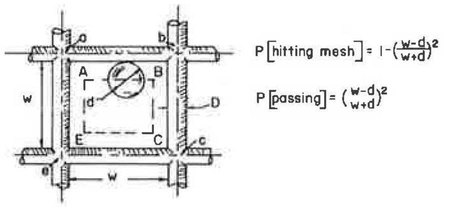

Figure 4. Example for locating particle in sample.

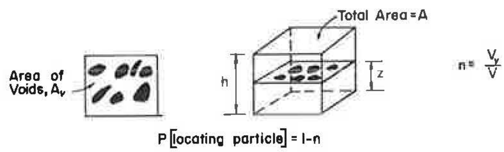

Figure 5. Three-step tree diagram.

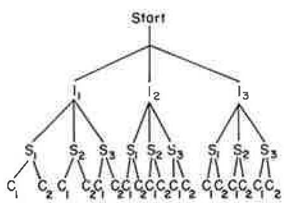

Figure 6. Probability of selecting favorable alternative = 1/24.

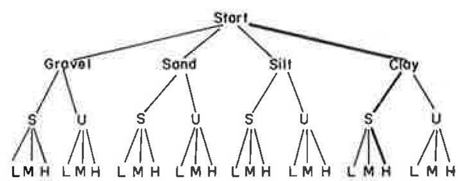

Figure 7. Probabilities of permutations.

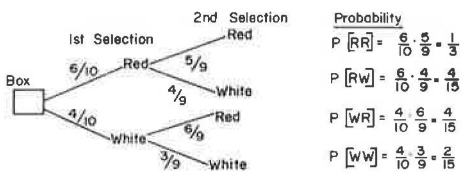

Figure 8. Venn diagram.

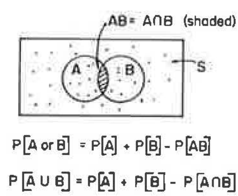

Figure 9. Scheme for determining the probability of impassable highway.

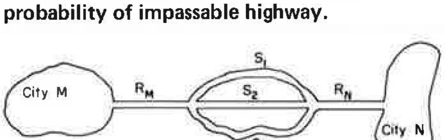

Highway	P[impossible]
R_M	0.6
R_N	0.5
S_1	0.4
S_2	0.7
S_3	0.9

Figure 10. Tree diagram of a posteriori probability.

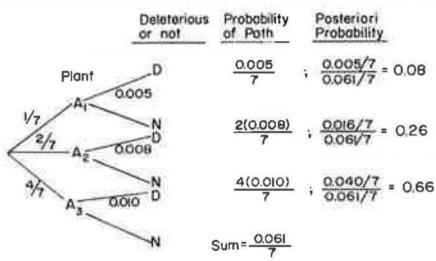

marked the beginning of the mathematical theory of inductive reasoning.

When written in the following form, equation 29 demonstrates how the introduction of the a posteriori outcome B alters the a priori assessment of the probability of A_i:

$$P(A_i|B) = P(A_i) \ \{\text{modification of } A_i \text{ when B is learned of}\} \tag{30}$$

where A_i are prior probabilities.

Aggregates used for highway construction are produced at three plants with daily production volumes of 500, 1,000, and 2,000 tons (450, 900, 1800 Mg). Past experience indicates that the fractions of deleterious materials produced at the three plants are 0.005, 0.008, and 0.010 respectively. If a sample of aggregate is selected at random from a day's total production and found to be deleterious, which plant is it likely produced the sample? Designate the following outcomes:

A_1 = production from the first plant, 500 tons (450 Mg) per day.
A_2 = production from the second plant, 1,000 tons (900 Mg) per day.
A_3 = production from the third plant, 2,000 tons (1800 Mg) per day.

The prior probabilities are

$$P(A_1) = \frac{500}{500 + 1{,}000 + 2{,}000} = 1/7$$

$$P(A_2) = \frac{1{,}000}{3{,}500} = 2/7$$

$$P(A_3) = \frac{2{,}000}{3{,}500} = 4/7$$

The likelihoods are

$$P(B|A_1) = 0.005$$

$$P(B|A_2) = 0.008$$

$$P(B|A_3) = 0.010$$

The joint occurrences are

$$P(A_1)\,P(B|A_1) = 1/7\,(0.005)$$

$$P(A_2)\,P(B|A_2) = 2/7\,(0.008)$$

$$P(A_3)\,P(B|A_3) = 4/7\,(0.010)$$

$$\text{Sum} = \Sigma P(A_i)\, P(B|A_i) = \frac{0.061}{7}$$

A posteriori probabilities are

$$P(A_1|B) = \frac{0.005/7}{0.061/7} = {}^{5}/_{61} = 0.08 \quad (0.14 \text{ a priori})$$

$$P(A_2|B) = \frac{0.016/7}{0.061/7} = {}^{16}/_{61} = 0.26 \quad (0.29 \text{ a priori})$$

$$P(A_3|B) = \frac{0.040/7}{0.061/7} = {}^{40}/_{61} = 0.66 \quad (0.57 \text{ a priori})$$

Because $P(A_3|B) = 0.66$ presents by far the greatest a posteriori probability, it is most probable that the deleterious sample came from the third plant. Of course, the same conclusion would be valid from a priori probabilities in this case. Figure 10 shows the tree diagram for this example. The a posteriori probabilities are obtained as the ratio of the probability of the required path to that of the sum of all paths that lead to a particular deleterious sample.

REFERENCES

1. J. R. Benjamin and C. A. Cornell. Probability, Statistics, and Decision for Civil Engineers. McGraw-Hill, 1970.
2. W. Feller. An Introduction to Probability Theory and Its Applications. John Wiley and Sons, 1957.
3. M. E. Harr. Influence of Vehicle Speed on Pavement Deflections. HRB Proc., Vol. 41, 1962.
4. M. E. Harr. Particulate Mechanics. In press.
5. T. C. Fry. Probability and Its Engineering Uses. D. Van Nostrand Co., 1965.

DISCUSSION

Richard L. Davis, Koppers Company, Pittsburgh

Traditional engineering education has had most calculations starting with assumptions without very much guidance on how to make valid assumptions. In nearly all engineering, these assumptions have grossly oversimplified the real conditions. This is particularly true of highway engineering where there is a great need to deal with real-world phenomena. I believe that Harr's paper can make an important contribution to this process for engineers. This is no easy task for the average engineer who usually views a test result for asphalt content of a mix as its true value rather than as a probability estimate of the true asphalt content. Familiarity with and use of probability methods will help to clarify and solve many baffling problems in highway engineering.

STATE OF THE ART IN PREDICTING THE PROBABILISTIC RESPONSE OF PAVEMENT STRUCTURES

B. Frank McCullough, University of Texas at Austin

Current design procedures that assume a homogeneous material do not account for the limited pavement distress that is experienced in the field; rather they are based on a catastrophic occurrence of distress. Variability of stress due to load variables and variability of pavement strength due to material characteristics are related in several recent developments, generally by making gross transformations between a statistical confidence level and satisfactory performance. Reliability techniques are described, and special attention is given to the Markov process. Reliability can be viewed as a probability that none of the following events occurs: (a) the number of overlays exceeds the allowed number; (b) the total cost of maintenance and overlays converted to net present value exceeds the allowed cost; and (c) a user delay penalty cost exceeds an allowed value.

•MATERIALS ENGINEERS recognize that the properties of the materials vary considerably from point to point in a specimen whether it is a steel bar or an asphalt surface. Figure 1, which is a continuous density profile for a crushed limestone base course, shows a typical dispersion of material properties in a pavement structure. Note that the density ranges in a random fashion from a low of 138 to a high of 147 lb/ft^3 (2210 to 2355 kg/m^3). The dispersion would be present for other material properties such as strength and modulus of elasticity, as well as for dimensions. Although these variations are recognized from a practical standpoint, current design procedures do not take this variation into account directly. Generally, design procedures assume a homogeneous material.

This type of approach assumes that distress is a catastrophic occurrence such that, when the stress exceeds a limiting value, a distress manifestation occurs. For example, the design premise for a static wheel load on a pavement is based on the assumption that if a limiting stress value is exceeded the entire pavement cracks. Experience and data from test roads indicate that this concept is contrary to what is observed in the field (1, 2, 3). Generally, pavement distress is experienced only over some percentage of the pavement area, and seldom does pavement distress appear throughout its length. Even on roads considered as a failure by engineers, the area of failure relative to the total area is small.

SIMPLE PROBABILITY TECHNIQUES

In recent years, several investigators and agencies have pointed to the need or attempted to take into account the stochastic process. The final report for NCHRP Project 1-10 pointed to the need for considering stochastic failure (4). In an independent study, Moavenzadeh and colleagues recognized the need and included stochastic processes in the development of the VESYS programs (5). The Texas Highway Department used stochastic processes in the development of its early versions of the flexible pavement system and rigid pavement system computer programs (6, 7).

The California Division of Highways (8) and the Asphalt Institute (9) in the development of their overlay design procedures considered variability of material properties by assigning a standard deviation to deflection values. McCullough in his overlay design procedure used probability analysis techniques to simulate the prediction of pave-

Figure 1. Continuous distribution of density of a crushed limestone base.

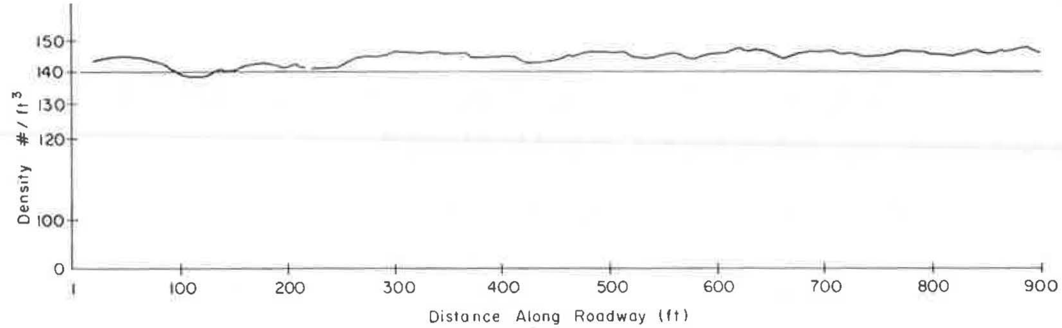

Figure 2. Probability of distress as a function of the dispersion of stress and strength density functions.

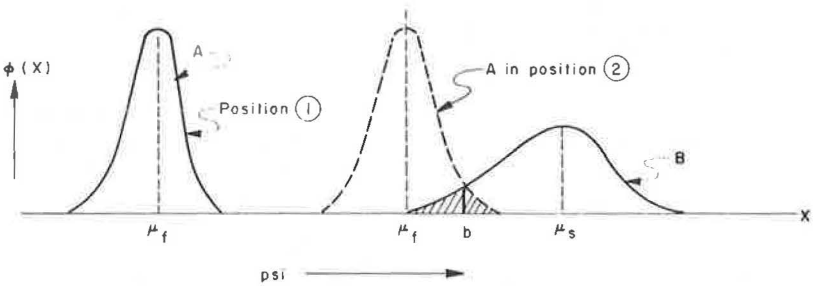

ment distress (10).

In the references, except for the VESYS program, probability techniques whether implied or stated were used in a design process to prevent the cracking (rupture) mode of distress. If the stress and strength variations in the pavement are characterized by normal distributions, then Figure 2 shows in a general fashion the fundamental hypothesis of these design methods. (A is the density function for stress and B the density function for strength in the specimen.)

If the dispersions of the stress and strength are clearly separated as is the case illustrated by position 1 in Figure 2 for the stress density function, then the material will perform satisfactorily without distress. The probability of distress in position 1 is zero. If the load, temperature, or moisture conditions change, then a shift of the stress density function to position 2 might be experienced; thus the probability of a failure assumes a finite value between 0 and 100 percent. Although the mean stress would still be less than the mean strength, a safe condition from a purely deterministic standpoint, distress will occur. Conceptually, the probability of distress may be expressed as the area beneath the intersection of curves A and B and is represented by the shaded area in the figure as follows:

$$P(D) = A \cap B \tag{1}$$

where P(D) = probability of distress. In Figure 2, the intersection of the two density functions may be designed as b on the psi axis. If the stress in a material is assumed to be independent of the strength, the probability of distress may be restated as follows:

$$P(D) = P(\text{stress} > b) + P(\text{strength} < b) \tag{2}$$

Each of the previously mentioned design methods takes variability into account by either quantifying equation 2 or making gross transformation between a statistical confidence level and satisfactory performance.

RELIABILITY TECHNIQUES

According to Darter and Hudson (11), "Reliability [of a pavement section] is the probability that the pavement system will perform its intended function over its design life and under the conditions (or environment) encountered during operation." They discussed the reliability of pavement design for a single performance period and touched on reliability considerations for pavements designed to be overlaid one or more times (11). The reliability and systems analysis of pavements of the second class are required to realistically simulate the long-term performance of a pavement structure.

Three approaches to simulation are reviewed on analytical grounds. Further empirical study may be needed to determine adequate approximating probability distributions required for implementation. The experimental needs and the particular sensitivity of reliability analyses on errors in the ad hoc distributions are briefly discussed.

SIMPLE RELIABILITY CALCULATION

Suppose a pavement is designed for k performance periods; i.e., it is designed to last for some time T assuming k - 1 overlays may be necessary. We are interested, then, in the probability that the life of the pavement exceeds T.

The following variables are used:

N_i = number of 18-kip (80-kN) loads before the ith overlay is required,
n = probability density function (pdf) of N_i, and
f_n = pdf of n.

Then the reliability is

$$P\left(\sum_{i=1}^{k} N_i > n\right) \tag{3}$$

where P( ) denotes probability.

The pdf of $\sum_{i=1}^{k} N_i$ is attainable by performing k - 1 convolution integrals (convolution via characteristic functions would probably be the most computationally efficient numerical approach):

$$f_{1,2}(N) = \int_0^{\infty} f_1(\xi)\, f_2(N - \xi)\, d\xi \tag{4}$$

where $N = N_1 + N_2$.

$$f_{1,2,\ldots,m}(M) = \int_0^\infty f_{1,\ldots,m-1}(\xi)\, f_m(M - \xi)\, d\xi \tag{5}$$

for m = 3, . . . , k - 1 where

$$M = \sum_{i=1}^{m} N_i$$

For convenience, $f_c = f_{1,2,\ldots,k}$.

Now a final convolution is required to obtain the pdf f_0 of $\sum_{i=1}^{k} N_i - n$.

Note that the pdf f_{-n} of -n is

$$f_{-n}(-n) = f_n(n)$$

Thus,

$$\begin{aligned} f_d(p) &= \int_0^\infty f_c(\xi)\, f_{-n}(p - \xi)\, d\xi \\ &= \int_0^\infty f_c(\xi)\, f_n(\xi - p)\, d\xi \\ &= \int_p^\infty f_c(\xi)\, f_n(\xi - p)\, d\xi \end{aligned} \tag{6}$$

Then, the reliability is simply

$$\int_0^\infty f_d(p)\, dp$$

Note that we have allowed for the possibility that the pavement may perform differently in different performance periods by treating f_i as different.

It is stated that n and N_1 are "believed to be" approximately lognormally distributed (1, pp. 35-36), from which we would suspect that the other N_i are also lognormal. Evidence for the normality of log N is stated to be available from fatigue tests, but further study is needed to verify that log n is normal.

The reliability analysis is particularly sensitive to errors in the distribution (12). Estimation of the probability of a rare event, abnormal failure, requires acceptable accuracy in the tails of the distributions; such accuracy generally requires larger samples than acceptable estimation of, say, the mean or variance.

The following example illustrates the problem. Suppose we have a sample size of 100. The mean estimate,

$$\bar{x} = \frac{1}{n}\sum_{i=1}^{n} x_i$$

is based on the entire sample and is relatively insensitive to moderate variations in small subsets of the sample. If the population variance is σ^2, then the variance of $\bar{x}$ is $\sigma^2/100$.

The estimate of the upper 0.05 point, however, is the sixth largest point (since 95 percent of the data are less than or equal to this value). Thus, sampling variations among the few largest data are not moderated by an averaging process that weights all data equally.

Regarding the age at failure (13), "Available data suggest that the relative frequency histograms may be approximated by a normal distribution function." Because the distribution of the number of 18-kip (80-kN) loads actually applied in a given period is not definitely known, the statement is not inconsistent with the belief that the number of loads to failure is lognormal.

If we approximate the time periods T_i for i = 1, 2, . . . , k of the k performance periods by normal distributions with respective means and variances μ_i and σ_i^2 for i = 1, 2, . . . , k, then the problem becomes very simple (3). The total lifetime of the pavement before the kth overlay is required is

$$T = \sum_{i=1}^{k} T_i \qquad (7)$$

T, then, is normally distributed with a mean of

$$\mu = \sum_{i=1}^{k} \mu_i$$

and variance of

$$\sigma^2 = \sum_{i=1}^{k} \sigma_i^2$$

Then the probability that the life T exceeds the design life T_D is the reliability:

$$P(T > T_D) = P\left(\frac{T - \mu}{\sigma} > \frac{T_D - \mu}{\sigma}\right) \qquad (8)$$

But $(T_D - \mu)/\sigma$ involves only constants, and $(T - \mu)/\sigma$ is normal with a mean of 0 and variance of 1. Thus, the reliability can be read directly from a table of values of the standard normal distribution function.

In the above, we have presupposed that the estimates to be used of μ and σ^2 involve sampling errors that are small compared to the standard deviation of T. This should be true, since the estimates $\hat{\mu}$ and $\hat{\sigma}$ are based on a sample, but T is a random variable whose variance is not reduced by averaging; e.g., T and $\hat{\mu}$ have respective variances σ^2 and σ^2/n where n is the sample size. Note that, if the sampling errors were not negligible, the problem would not simply involve computing the upper confidences of a t-statistic. The simplest solution in this case would be to replace μ and σ with $\hat{\mu}$ and $\hat{\sigma}$ in the above analysis to obtain an approximate reliability estimator. Alternatively,

$$p(T > T_D) = p(T - \hat{\mu} > T_D - \hat{\mu}) = p\left(\frac{T - \hat{\mu}}{\hat{\sigma}\sqrt{1 + \frac{1}{n}}} > \frac{T_D - \hat{\mu}}{\hat{\sigma}\sqrt{1 + \frac{1}{n}}}\right) \tag{9}$$

The variable on the left is a t-statistic, and the variable on the right does not have a known, simple distribution. Similarly,

$$p(T > T_D) = p\left(\frac{T - T_D}{\hat{\sigma}} > 0\right) \tag{10}$$

and the statistic does not have a t-distribution, because the numerator does not have mean 0, unless $E(T) = T_D$, in which case the reliability is 0.5.

This is not cause for alarm, inasmuch as the approximate reliability obtained by replacing μ and σ by $\hat{\mu}$ and $\hat{\sigma}$ should be acceptable unless $\hat{\mu}$ and $\hat{\sigma}$ have sampling errors that are not small compared to σ (the standard deviation of T), in which case the reliability calculation would be suspect anyway.

MARKOV CHAIN MODEL

McCullough and Hudson (4) discussed a clever approach for performing reliability analyses of single-performance pavements by using a Markov chain model. The four states of the pavement are

1. Normal aging,
2. Accelerated aging, "a state caused, for example, by the initiation of cracking or surface polishing,"
3. Maintenance, and
4. Failure.

The transition matrix is the matrix of probabilities of one-step transition among states. Transition matrices are suggested for four cases:

1. Standard operating procedures,
2. High maintenance activity, standard quality,
3. Standard maintenance activity, high quality, and
4. High maintenance activity, high quality.

The matrix for case 1 is

$$P_I = \begin{pmatrix} 0.95 & 0.05 & 0 & 0 \\ 0 & 0.40 & 0.20 & 0.40 \\ 0.60 & 0.30 & 0 & 0.10 \\ 0 & 0 & 0 & 1 \end{pmatrix}$$

Thus, according to the first row the probability of remaining in state 1 in time step i, given that the pavement is in state 1 in step i - 1, is 0.95. The probability of passing from state 1 to states 2, 3, and 4 is 0.05, 0, and 0 respectively. In general, the one-step probability of passing from state i to state j is the (i, j) element of the matrix.

Then, the reliability is the probability of not reaching state 4 in the design lifetime. If ρ is the vector of probabilities of initial states and P is the transition matrix, it can be shown that ρP^n is the vector of state probabilities after n transitions. Then one minus the fourth element of ρP^n is the reliability if n/2 is the design life in years, since the time step is one-half year.

The model can be generalized to handle the multiple-performance-period case by altering the state space, as follows:

1. Normal aging, period 1,
2. Accelerated aging, period 1,
3. Minor maintenance, period 1,
4. First overlay,
5. Normal aging, period 2,
6. Accelerated aging, period 2,
7. Minor maintenance, period 2,
8. Second overlay, etc.

If the number of performance periods is k, then there are 4k states, the 4kth state being failure. If the design life is n/2 years, then the reliability is one minus the 4kth element of ρP^n.

In this approach, we have obviated estimation of the tails of distributions. However, moderate errors in the transition probabilities could cause large errors in the P^n matrix if n is large. Thus, accurate estimation of the transition probabilities is important. The possibility of drift in the P matrix as traffic patterns change is a difficult problem that should be considered.

High maintenance probabilities, especially over an extended period of time, are of practical interest because of their relationship to direct costs and user inconvenience. Moreover, the likelihood of frequent maintenance during key periods, e.g., just before expected overlay times, might signify the need for a decision policy alteration.

The desired probabilities are easily attainable from the model; the (4m - 1) th element of ρP^n is the probability of being in maintenance in the mth period at time step n.

Extended periods of high probabilities of being in a state associated with low serviceability are similarly of interest. Note that, by altering the transition probabilities to the maintenance and overlay states, we can study the sensitivity of direct maintenance and user delay costs and serviceability to rehabilitation policies. The sensitivity of the system to maintenance quality can be studied by varying the transition probabilities from the maintenance state. The sensitivity to overlay quality can be seen by varying the transition probabilities after the first overlay. Effects of random errors in the transition probabilities should also be studied via sensitivity analysis. It is clear that the Markov chain model yields much more information than a simple reliability calculation.

The undesirability of the uniform step size and allowance for a single state for an entire section is apparent. The disadvantages can be reduced by using a finer step size and a more detailed state space.

MARKOV PROCESS MODEL

We now consider a model in which time is continuous and the section is divided into several subsections of, say, 100 ft (30 m). For illustration, we consider the four states of the Markov chain model, but a state is associated with each subsection.

The Markov process model is suggested because of the extensive information that can be obtained from it; the policy and sensitivity analyses mentioned in conjunction with the Markov chain model can be carried out in more detail with the Markov process model.

The more sophisticated model, however, requires more extensive inputs, as is apparent from the discussion below; thus, the extra demands in experimentation to determine the inputs should be weighed against the advantages.

Because of the complexity of the model, digital simulation is suggested as a solution technique. Development of a computer program would be greatly facilitated by the use of a simulation language such as GASP (5). The elements of the simulation model are described below.

1. Randomly determine the initial state of each subsection as normal aging or accelerated aging.
2. For each section, randomly determine the time in the initial state and the state next to be occupied.
3. Upon transition of a section, randomly determine the time to remain in the new state and the state next to be occupied. After each transition, test whether it is time for an overlay by examining the states of all subsections and applying predetermined decision criteria; e.g., compare the percentage of subsections in the accelerated aging state to a threshold percentage.
4. If an overlay is indicated, randomly determine the time required for the overlay. After the overlay, repeat steps 1 through 3. Continue the entire process until the allowed number of overlays has been exceeded or the design life is completed.

The interrelations among events must be considered. For example, the transition of a subsection after an overlay could be a function of

1. The a priori probabilities of state transitions and distribution of the time in the state to be transferred from,
2. The states of nearby subsections, or
3. Convenient measures of the performance of the subsection before the overlay.

The following hypothetical list of events illustrates the basic information that is available from the simulation for analysis.

Time (months)	Event
0	Begin simulation; all subsections aging normally
20	Section 6 enters accelerated aging state
23	Section 23 enters accelerated aging state
26	Section 6 enters maintenance
26.05	Section 6 enters normal aging state ($1\frac{1}{2}$ days required for maintenance)
⋮	
128.7	Section 47 enters accelerated aging state; percentage of sections in accelerated aging state exceeds threshold value; begin overlay
⋮	

Thus, detailed statistics could be collected on things such as maintenance costs, maintenance time, and percentage of sections in accelerated aging at any given time.

As with the Markov chain model, sensitivity analyses should be performed to determine (a) the effects of varying the overlay and maintenance policies and (b) the effects of random errors in the empirically determined inputs.

A straightforward measure of reliability is the probability that the number of overlays exceeds the allowed number in the design life. Alternatively, reliability can be viewed as the probability that none of the following events occurs:

1. The number of overlays exceeds the allowed number,
2. Total cost of maintenance and overlays converted to net present value exceeds the allowed cost, and
3. A user-delay penalty cost exceeds an allowed value.

SUMMARY

The state of the art of predicting pavement probabilistic response may be summarized as follows:

1. Most of the early work and the currently implemented methods considering variability use simple probabilistic techniques to simulate performance;
2. Recent studies have been oriented toward approximating the complex multivariate distributions of material properties and pavement dimensions to achieve a stochastic prediction of performance; and
3. Future work should be directed along the thrust of item 2 considering that a pavement life will consist of the initial performance period plus numerous overlays.

REFERENCES

1. Road Test One-MD, Final Report. HRB Special Rept. 4, 1952.
2. The WASHO Road Test, Part 2. HRB Special Rept. 22, 1955.
3. The AASHO Road Test: Report 5—Pavement Research. HRB Special Rept 61E, 1962.
4. B. F. McCullough and W. R. Hudson. Translating AASHO Road Test Findings—Basic Properties of Pavement Components. Materials Research and Development, Inc., 1970. (Also published as W. R. Hudson and B. F. McCullough. Flexible Pavement Design and Management—Systems Formulation. NCHRP Rept. 139, 1973.)
5. F. Moavenzadeh et al. Rational Design of Flexible Pavements: The PADS Model. M.I.T., Research Rept. R74-26, 1974.
6. J. E. Orellana. FPS-11 Flexible Pavement System Computer Program Documentation. Texas Highway Department; Texas Transportation Institute, Texas A&M Univ.; and Center for Highway Research, Univ. of Texas at Austin, Research Rept. 123-15, April 1972.
7. R. K. Kher, W. R. Hudson, and B. F. McCullough. A Systems Analysis of Rigid Pavement Design. Texas Highway Department; Texas Transportation Institute, Texas A&M Univ.; and Center for Highway Research, Univ. of Texas at Austin, Research Rept. 123-5, Nov. 1970.
8. E. Zube and R. Forsythe. Flexible Pavement Maintenance Requirements as Determined by Deflection Measurements. Highway Research Record 129, 1966.
9. Asphalt Overlays and Pavement Rehabilitation. The Asphalt Institute, Manual Series 17, Nov. 1969.
10. B. F. McCullough. A Pavement Overlay Design System Considering Wheel Loads, Temperature Changes, and Performance. Univ. of California, Berkeley, PhD dissertation, July 1969.
11. M. I. Darter and W. R. Hudson. Probabilistic Design Concepts Applied to Flexi-

ble Pavement System Design. Center for Highway Research, Univ. of Texas at Austin, Research Rept. 123-18, 1973.
12. R. G. Sexsmith and M. F. Nelson. Limitations in the Application of Probabilistic Concepts. Journal of American Concrete Institute, Oct. 1969, pp. 823-828.
13. B. F. Hutchinson. A Conceptual Framework for Pavement Design Decision. Highway Research Record 121, 1966, pp. 1-14.
14. A. C. Lemer and F. Moavenzadeh. Reliability of Highway Pavements. Highway Research Record 362, 1971, pp. 1-8.
15. A. A. Pritsker and P. I. Kiviat. Simulation With Gasp II. Prentice-Hall, 1969.

MATHEMATICAL ANALYSIS OF PAVEMENTS WITH NONUNIFORM PAVING MATERIALS

E. J. Barenberg, P. F. Wilbur, and S. D. Tayabji,
University of Illinois at Urbana-Champaign

The variability of paving materials and the effects of such variations on the behavioral responses of pavement systems are evaluated. Methods for evaluating the effect of material variability on pavement system responses are presented and analyzed. Analyses are presented that evaluate the characteristic variations in components of pavement systems and methods of quantifying them. Factors such as the severity and location of variations are evaluated, and sensitivity analyses are performed to determine the relative and real effects of specific types, locations, and severities of the variations on pavement system responses. The paper discusses the relationship between the variability observed when discrete specimens of a material are tested and the variability of a continuum constructed from the same material. The importance of eliminating testing error and similar sources of error when the continuum is evaluated is emphasized. Monte Carlo simulation and other techniques are applied to obtain a pattern for pavement system responses on pavements with specific types of variations and loading conditions. Results show that the variability of the paving materials can have a profound effect on the responses of the pavement to load, especially to strain response, and that the location and extent of the variation are critical with respect to the response. Also, the Monte Carlo simulation technique for predicting the range of responses is limited unless a very large number of analyses are used in the simulation.

•LITTLE is known about the manner in which the nonuniformity of paving material properties and subgrade support affect the behavior and response of pavement systems to loads. Pavement systems do exhibit significant variations in response to loads, but the extent to which this variability is influenced by variations in material properties in different pavement components is not known (1, 2, 3, 4).

Laboratory test results from prepared specimens of paving materials show substantial variability in material properties. There are, however, several problems associated with using the variability from tests on discrete specimens to predict the variability of materials in pavement systems. One problem is that most test specimens are made up outside the pavement system. Thus, the variability observed in these test results may not reflect the true variability of the material in the pavement system. This is especially critical in the case of compaction because procedures for compacting materials in the pavement are completely different from those for compacting test specimens and most materials are highly sensitive to their compacted density.

Another problem in correlating the variability of test results from control test specimens and the material in the pavement is that the results from test specimens are influenced by the edge conditions of the specimen and by specimen size; the materials in the pavement are continuous. Because material in the pavement is continuous, there is probably a gradual transition in the material properties within the pavement system; the material in a test specimen is probably more uniform throughout the specimen but is affected by the specimen boundaries. Also, the variability of results from control specimens may be different from the corresponding variability of the material in the pavement because of the relative quantities of material involved. The response of the pavement system is influenced by properties of the material, but the pavement system includes a much greater volume of material than normally included in control specimens. Thus, the area of influence that affects the response of the pavement must be considered in any analysis of pavement variability.

Laboratory testing is, of course, the only available method for evaluating material properties. Thus, the variability in test results from laboratory specimens must ultimately be reconciled with the variability of in situ materials or, more importantly, with variability in the responses of pavement systems to external stimuli. One method of reconciling these two factors is by inference, that is, by evaluating the effect of material variability on the response of pavement systems and by correlating calculated material variability from pavement responses with measured variability of control specimens. This, of course, requires models that can be used to evaluate the effects of material variability on pavement responses. With such a model, the effects of variability in the various pavement components can be evaluated. By using models capable of handling nonuniform material characteristics in the various pavement components, it will be possible to perform sensitivity analyses to establish the relative effects of changing levels of material variability on pavement response.

One problem with using mathematical models to evaluate these responses is that a data base must be developed for statistical analyses of the response of pavement systems. The problem is one of specifying the critical distributions of strong and weak areas through the pavement system so that the analyses will provide realistic indications of the worst and best possible conditions. If only static loads were applied, the probability of a load being applied at the most critical location with respect to pavement weaknesses could be remote. With moving loads, however, the likelihood of a load or loads being applied at the most sensitive locations becomes much greater. For example, if an area of weak subgrade support exists near the edge of a pavement, then it seems likely that the worst condition would be application of a load to the pavement directly over the location of the weak support, and there is a high probability that moving loads will pass over this critical location. Thus, not only must a statistical evaluation be made of the pavements, but the most likely worst conditions must also be identified and analyzed.

The purpose of this paper is to evaluate procedures for analyzing pavement systems with nonuniform paving material properties. Statistical procedures for assigning critical properties to the paving materials at specific locations are evaluated, the pavements are analyzed with the assigned properties, and the results are compared with what are considered to be the best and worst combinations of material properties for the pavement system. Analysis of the pavement system is done with a finite element model. Results of analyses of pavement systems with various levels of material variability are compared and evaluated.

APPROACH

In an earlier paper, Levey and Barenberg (5) showed how numerical analysis models can be used to evaluate the effects of nonuniform paving materials on pavement responses. They demonstrated that the stresses, strains, and deformations of the pavement system were clearly affected by variability of the paving material and by the size and distribution of the variations within the pavement system. Their results clearly showed that a normal distribution of responses could be expected with paving materials having a normal distribution of properties.

They used a two-dimensional numerical model to evaluate a pavement system and concluded that the three-dimensional case could also be analyzed if sufficiently large high-speed computers were available or if models that represent the pavement system in three dimensions were more efficient (5). Inasmuch as computer capacity has remained nearly constant since that paper was prepared, a direct analysis of the three-dimensional pavement system with nonuniform material properties is still not practical.

Several existing models were evaluated to find the model best suited for this analysis. Included in the evaluation were the finite element model for the analysis of pavement slabs developed by Hudson and Matlock (6, 7) and the basic finite element models developed by Wilson (8). The model chosen for the study was a finite element model developed by Eberhardt (9) for analysis of two-layered slabs on a Winkler type of support. The Eberhardt model was chosen for several reasons. Because of time and resources, only one type of pavement could be analyzed. Inasmuch as rigid pavements have fewer variables with more clearly defined material properties, they were chosen for the evaluation. Also, finite element models were available to consider rigid pavements as a three-dimensional problem whereas the models applicable with flexible pavements more nearly represent a two-dimensional analysis of these systems. Thus, it was decided to use a finite element model that represents a continuously supported slab rather than a more generalized finite element model such as the model developed by Wilson (8) and modified by others. The above decisions reduced the choice of models to essentially the Hudson and Matlock model (6, 7) and the Eberhardt model (9). The Eberhardt model was selected because, when we verified the models, it gave stresses closer to those obtained with the elastic slab theory and it was capable of evaluating two-layered as well as single-layered slabs. Although two-layered slab systems were not evaluated in this study, the model can analyze such systems, and this capability permits evaluation of variable thicknesses of a subbase under the concrete slab.

The rectangular plate element shown in Figure 1 is used to represent the pavement slab. Each slab is made up of a number of such elements, and the loaded configuration of each element is defined in terms of the corner nodes of each element. Displacement of the nodal points is interpreted as actual displacement of corresponding points in the pavement system. The varying stress field in each element is defined by an equivalent set of discrete-element forces acting at the corner nodes. These fictitious element forces have no real physical counterpart but simply approximate the varying stress field in the real pavement system. The displacements of the corner nodes are described by three components: vertical displacement W (z-direction), rotation about the x-axis (θ_x), and rotation about the y-axis (θ_Y). Figure 1 shows the positive displacement components. The procedure for developing the element stiffness matrix (9) was based on the classical theory of thin plates.[1] The final force-displacement equations for a plate element can be written as

$$\{F\}_e = (k)\ \{D\}_e \tag{1}$$

where (k) is a 12*12 plate element stiffness matrix relating the nodal displacement vector $\{D\}_e$ to the nodal force vector $\{F\}_e$.

SUBGRADE STIFFNESS MATRIX

The subgrade support is defined by a grid identical in size, pattern, and location to the grid used to define the slab elements. The two grid systems are aligned so that they coincide at all nodal points.

Energy principles were used to develop the force-deformation relationships for the subgrade support. The subgrade stiffness matrix was established by applying successive virtual unit displacements at each of the four nodal points of the plate elements, and the force-displacement equations for the plate and the subgrade element were obtained by equating the sum of the internal and external work to zero; i. e.,

$$\{F\}_e = [(k) + (k_s)]\ \{D\}_e \tag{2}$$

[1] Information on development of a finite element model was submitted with this paper as an appendix and is available in Xerox form at the cost of reproduction and handling. When ordering, refer to XS-64, Transportation Research Record 575.

where (k_s) is a 12*12 stiffness matrix for the subgrade support element.

The global force-displacement equations for a finite element grid (Figure 2) can be written as

$$\{F\}_g = (K)_g \{D\}_g \tag{3}$$

where

$\{F\}_g$ = vector containing all the global forces,
$\{D\}_g$ = vector containing all global displacement, and
$(K)_g$ = global stiffness matrix.

Equation 3 is solved for $\{D\}_g$ and subsequently for strains (ϵ_{XX}, ϵ_{YY}, ϵ_{XY}) and stresses (σ_{XX}, σ_{YY}, σ_{XY}). Eberhardt (9) verified the finite model by comparing the results obtained by using this model with theoretical results from equations developed by Westergaard. Good agreements were obtained for both deformation and stresses.

In the model developed by Eberhardt, the stiffness of the pavement was assumed to be uniform, and stiffness values for all elements were assigned as a constant value. For this study, the computer program written by Eberhardt was modified so that specific values of the flexural rigidity D are assigned to each element so that the rigidity of the slab is varied in a random manner. Similarly, specified values for the subgrade support k are assigned for each subgrade element so the subgrade support can also be varied in a random manner.

INCORPORATION OF VARIABILITY

For isotropic slab materials assuming a state of plane stress, the 3*3 matrix (D) represents Hooke's law for two-dimensional stress problems as follows:

$$(D) = \frac{Et^3}{12\,(1 - \nu^2)} \begin{pmatrix} 1 & \nu & 0 \\ \nu & 1 & 0 \\ 0 & 0 & \frac{1-\nu}{2} \end{pmatrix} = D(N) \tag{4}$$

where

E = elastic modulus,
t = plate thickness, and
ν = Poisson's ratio.

Thus, from equation 4,

$$(N) = \begin{pmatrix} 1 & \nu & 0 \\ \nu & 1 & 0 \\ 0 & 0 & \frac{1-\nu}{2} \end{pmatrix}$$

and

$$D = \frac{Et^3}{12\,(1 - \nu^2)} \tag{5}$$

The matrix (D) is used in formulating the plate element stiffness matrix (K).

The material variability is incorporated into this model by multiplying the matrix (D) described in equation 4 for each element by a random number R from a set that has a mean value of unity and a specified coefficient of variation. Then

$$(D') = RD(N) \tag{6}$$

where (D′) is the modified (D) matrix. For the purpose of this paper R is assumed to reflect the variability in the modulus value E of the plate. However, as can be seen from equation 4, R can also be considered to reflect the variability in D, the flexural rigidity of the plate, which includes the variability in the plate thickness t as well as the variability in E.

GENERATION AND ASSIGNMENT OF RANDOM VARIABLES

A program that generates random numbers was described by Levey and Barenberg (5) and Levey (10). This program can produce sets of random numbers with normal distributions having specified means and standard deviations. This program was used to generate sets of R-values, which were assigned to the elements in a random pattern. Two methods were used to select the sets of random values used in the analysis.

One method of assignment was basically a Monte Carlo simulation procedure in which the values in the sets were generated and assigned to the model elements in a random manner and the system was analyzed with the randomly assigned values. The difficulty with this procedure is that it is not known whether arrangement of the randomly assigned values produced a pavement response that was better or worse than a mean response and to what extent. Thus, with this approach, it is necessary to make enough separate assignments and separate analyses so that the results can be analyzed statistically. A large number of independent runs of this type are required to develop the necessary background data for a statistically based analysis of the response characteristics of the pavement system. In the earlier work by Levey and Barenberg (5), 20 such independent analyses were made in the Monte Carlo simulation of the pavement response characteristics. Although this number appeared adequate, there is no sure way of determining the accuracy of the statistical parameter without developing larger data bases. Large data bases require substantial funds for computer costs and analyses.

Because of the high computer costs and the uncertainty when the Monte Carlo technique is used to establish the responses of pavement systems, an alternate method was used to determine the range of responses that could be expected from a pavement with a specified degree of nonuniformity of paving materials. The random number generator was used to generate sets of values for the specific property under investigation, and the sets were assigned to specific numbered elements of the pavement slab. Approximately 50 sets were generated, and the results were studied to determine which sets of values would likely produce the best and worst pavement responses. Figure 3 shows the numbered pavement elements and the location of loads near the corner and edge of the pavement. Figure 4 shows the values for modulus of elasticity of the slab material to produce the anticipated best and worst pavement responses for the edge loading condition. Figure 5 shows information for the subgrade support k. Both sets of values have a coefficient of variation of 30 percent. Notice that, for both the modulus of elasticity of the slab and the subgrade support, the values assigned to the four elements surrounding the loaded area are significantly higher or lower than the average values. Because all values were assigned to the elements in a random manner and the sets of values for the best and worst conditions were selected from a large number of randomly generated sets, results with these values should provide an excellent indication of the range of responses that could be expected if a full Monte Carlo simulation were made.

Because this latter approach required much less computer time than the full Monte

Figure 1. Rectangular plate element.

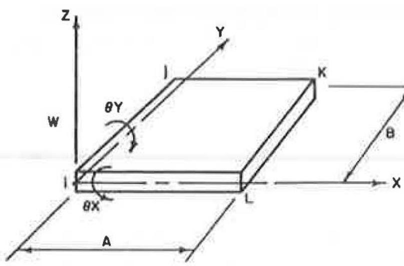

Figure 2. Finite element grid for assembling global stiffness matrix.

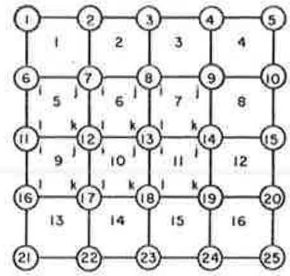

Figure 3. Numbered pavement elements and location of edge and corner loads.

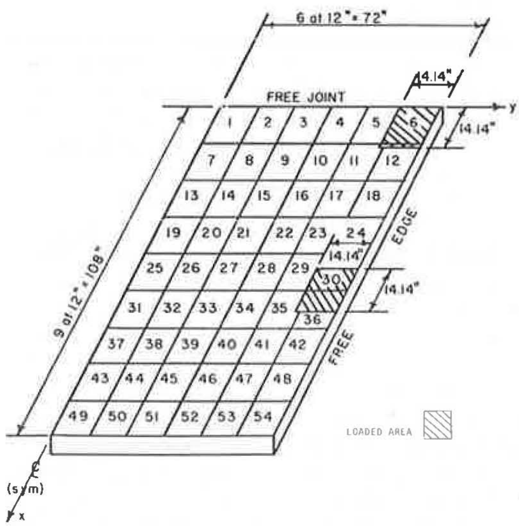

Figure 4. Pavement elements with the randomly assigned values for slab modulus.

4237	4413	5534	5385	4883	3541	
4987	4121	5516	4760	4330	7888	
3902	3913	3978	6976	3394	5789	
5383	4186	2017	4452	3382	2761	
4723	5048	5518	4555	4883	2503	
4424	4379	5082	3780	2636	3842	
2097	4440	3158	3963	3398	3966	
5134	2294	4499	2719	3964	4061	
2756	5566	5959	912	3761		4773
2505	4743	5564	3303	2942		1686
3551	2576	4785	5158	5669		5774
2528	4358	2960	3000	2444		427
5569	4451	4781	4207	3083	3261	
5379	6109	2394	3002	4436	4630	
4938	3388	3537	3220	3537	6461	
4558	4102	4005	4194	5064	5218	
4943	5422	4018	3350	3204	3622	
4701	4206	2876	3385	4613	3677	
4889	5780	4330	3168	2974	4163	
3556	5229	4379	4179	4545	4260	

Figure 5. Pavement elements showing the subgrade support values in lb/in.^{3}.

106 125	110 103	139 137	135 119	122 108	86 197	
97 135	98 105	99 50	175 111	88 95	145 69	
118 111	126 110	138 127	114 94	122 66	63 96	
52 128	111 57	79 115	99 68	85 99	99 102	
69 63	139 119	149 139	23 83	94 74		119 42
89 63	64 109	120 74	129 75	142 76	144 61	
139 11	111 135	119 153	105 60	77 75	81 111	
123 116	85 114	88 103	81 100	88 105	161 127	
124 130	136 118	100 105	84 72	80 85	91 92	
122 89	145 131	108 110	79 105	74 114	104 107	

Carlo simulation, it was used to study the effects of material variability and load position on the pavement response. A limited Monte Carlo simulation was also made to show the similarity and differences that can be obtained with the two procedures.

In these analyses only one parameter was varied at a time. Thus, when the effects of the slab modulus were evaluated, the subgrade was held uniform. Similarly, when the effects of variability of the subgrade were evaluated, the slab modulus was held uniform. The pavement system responses were evaluated for both edge and corner load conditions. All loads were 10,000-lb (4540-kg) wheel loads with a contact pressure of 50 psi (345 kPa) assumed to be uniformly distributed over the loaded area.

RESULTS

The computer program used in the analysis provided all typical pavement responses such as deflections, stresses, and strains at all locations specified. However, only a limited amount of these data are presented here. Strain in the pavement slab was chosen as the parameter for presentation and analysis here because it represents a critical response in the performance of concrete pavements (4) and appeared to be the most sensitive to changes in paving material variability.

Figures 6 and 7 show the strains in the x- and y-directions for pavement systems with uniform paving materials under corner and edge loading conditions respectively. Note that for the corner loading condition the critical strains are not under the load. Similarly, for the edge loading condition the maximum strain in the x-direction (ϵ_X) occurs under the load, but the maximum strain in the y-direction (ϵ_Y) occurs away from the loaded area, indicating a cantilever effect in the y-direction. Under the edge load, the strain in the x-direction ϵ_X is significantly greater than the strain in the y-direction ϵ_Y. These results are consistent with results from closed form solutions such as the Westergaard model.

Figures 8 and 9 show the difference in ϵ_X and ϵ_Y for the best and worst conditions under edge loading as the coefficient of variation for the modulus of elasticity of the slab material increases from 10 to 30 percent. Reasons for change in the shape of the curves between the best and worst conditions can be seen by studying the patterns of the assigned moduli values in Figure 4. In particular, the area of weakest material does not generally coincide with the points of maximum strain. Thus, as expected, when the variability in the moduli values increased, as with the higher coefficients of variation, the point of maximum strain tended to move toward the area of low bending resistance. A similar set of curves for the corner load condition is shown in Figures 10 and 11, and the same trends exist.

A Monte Carlo simulation of the responses under edge and corner loads was made, and the statistical parameters were calculated. Figures 12 and 13 show the differences obtained for ϵ_X and ϵ_Y under edge loading by using the Monte Carlo simulation with 10 repetitions. The results from analyses with the designated best and worst conditions are also shown for comparison. There are significant differences in the range of values obtained by the two methods. Figure 14 shows a statistical summary of ϵ_X obtained from the two approaches.

Because of the significant differences obtained when the Monte Carlo simulation techniques were used compared with the designated best and worst conditions, it is well to review again the differences in these two approaches.

In the Monte Carlo simulations, the appropriate moduli values were generated and assigned to numbered elements on a random basis. Then the system was solved and the responses of that system were recorded. A new set of random moduli values, with the appropriate mean and standard deviation, was then generated and assigned, and the system was again solved for responses. After a specified number of repetitions (in this case 10), pavement responses were analyzed to determine the statistical characteristics of these responses. Only 10 repetitions were made because of the computer costs involved for each solution and the limited funds available.

The designated best and worst conditions for the pavement responses were determined in the following manner. First, a number of sets of random values were gen-

Figure 6. Location and magnitude of strains in the x- and y-directions for a pavement with a corner load and uniform support.

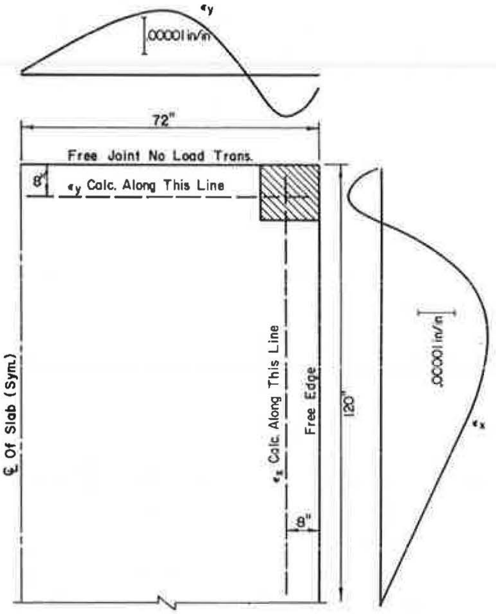

Figure 7. Location and magnitude of strains in the x- and y-directions for a pavement with an edge load and uniform support.

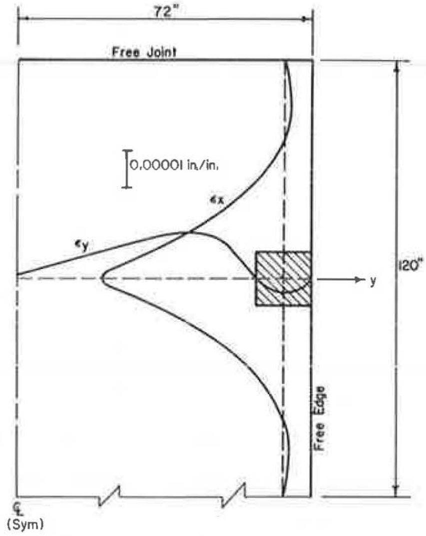

Figure 8. Effect of variability of slab modulus on the strains in x-direction due to edge loading.

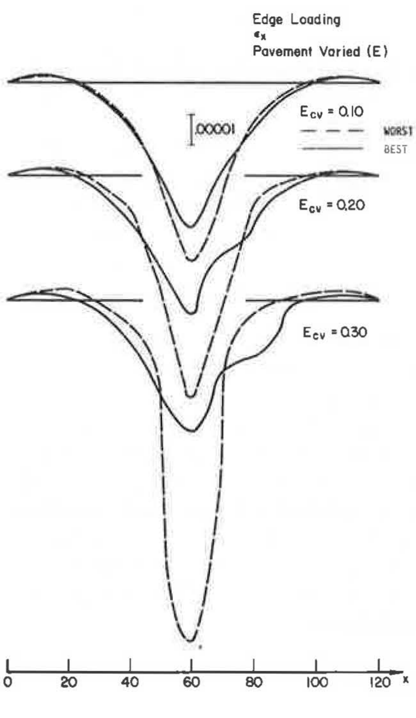

Figure 9. Effect of variability of slab modulus on the strains in y-direction due to edge loading.

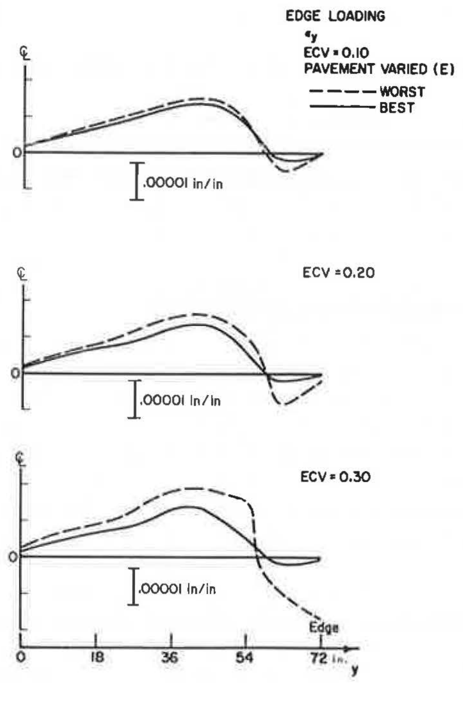

Figure 10. Effect of variability of slab modulus on strains in x-direction under corner loading.

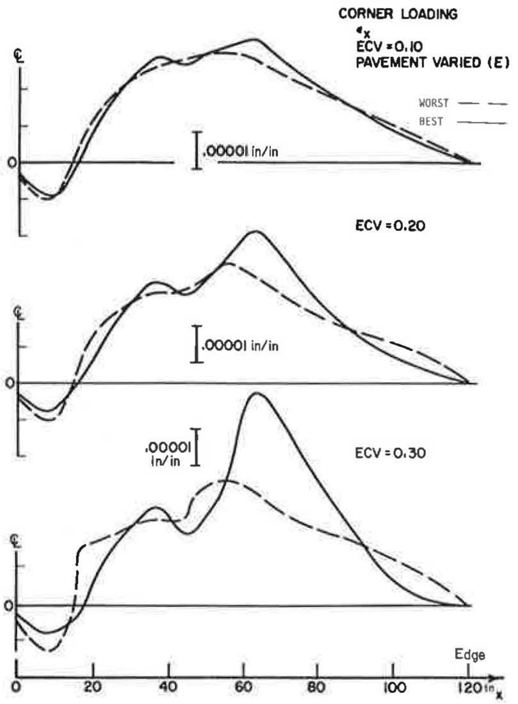

Figure 11. Effect of variability of slab modulus on strains in y-direction under corner loading.

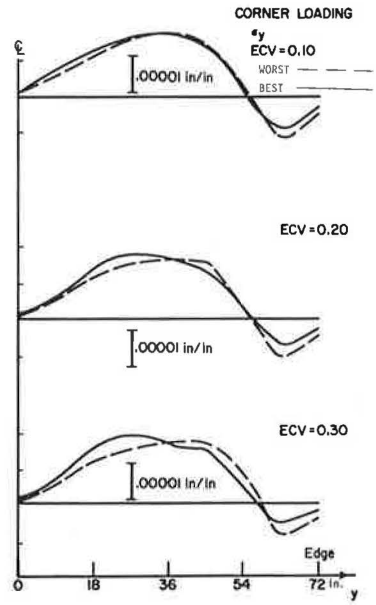

Figure 12. Variations in x-direction strains due to variations in the pavement.

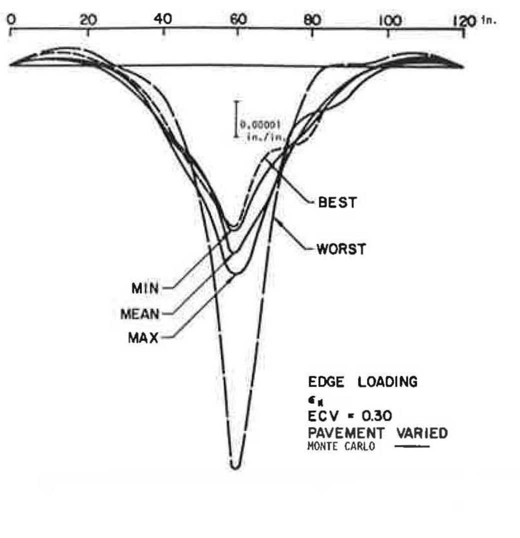

Figure 13. Variations in y-direction strains due to variations in the pavement.

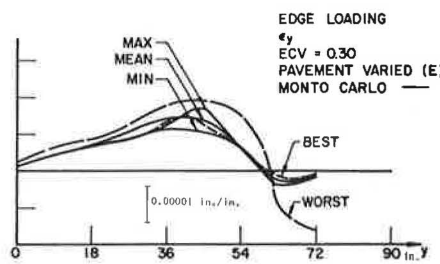

Figure 14. Comparison of ranges in maximum strains due to edge loading.

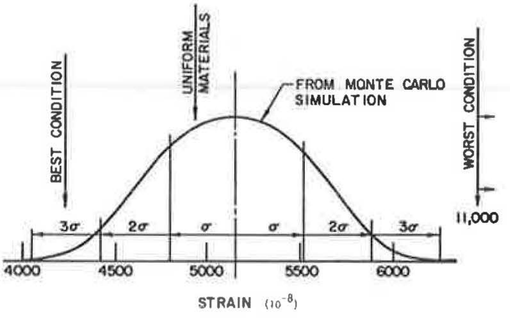

Figure 15. Variations in strains in y-direction due to variations in the subgrade for pavements under edge loads.

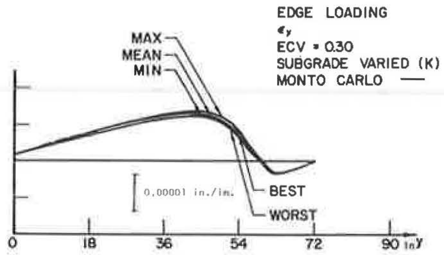

Figure 16. Variations in strains in x-direction due to variations in the subgrade for pavements under corner loads.

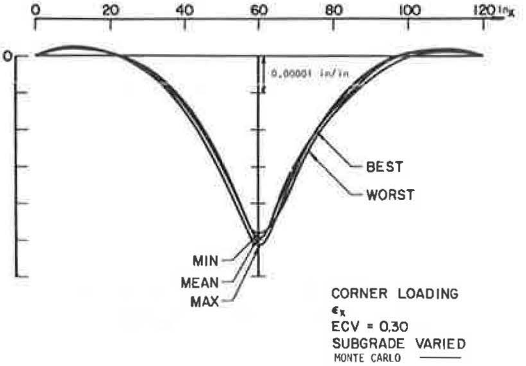

Figure 17. Ranges in maximum strains due to edge loading caused by variations in the subgrade.

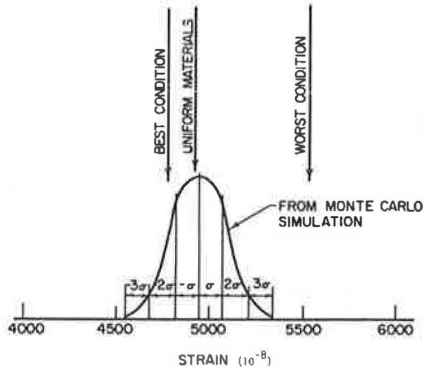

erated and listed sequentially. These sets were then studied to find the one that had four values in critical relative positions that were significantly less than average. The values in the desired set were then shifted as a unit such that all values remained in the same relative position sequentially but that the four smallest values grouped together would be assigned to the four elements directly under or surrounding the loaded area. Similarly, the sets of generated values with the highest E-values grouped together were assigned to fall under and around the loaded area to produce the best condition.

It is believed that the above method of establishing the best and worst conditions is valid because all randomly generated values were allowed to remain in their same relative position, but the entire set was shifted so that the weakest and strongest regions of the pavement coincided with the critical loaded area. For pavements in normal service, the location of the strong and weak areas would, of course, remain fixed, but the loads could move so that eventually the load would occur over the strong or weak areas of the slab. Thus, the method used for determining the best and worst condition appears reasonable, and this information can be obtained for significantly less computer expense than with the Monte Carlo simulation.

The effects of varying the subgrade support while holding the modulus E of the paving material constant were not so dramatic as the effects of varying the moduli of the paving materials. A summary of the results using both methods of analysis is shown in Figures 15, 16, and 17. The low sensitivity of the pavement responses to varying subgrade properties is surprising to the authors, especially since the total pavement deflection also proved to have a low sensitivity to the variability in the subgrade support.

Because time and money were limited, the effect of the size of the softer area of the subgrade on the pavement response was not evaluated. Variations in the subgrade for this analysis were assigned element by element. Because each element covers only 1 ft^2 (0.09 m^2), a loss of support over an area of this size may not significantly affect the response of the pavement system. Then the worst condition was evaluated, the set of values with the lowest average k for the four elements around and under the loaded area was used. Again, the area of 4 ft^2 (0.37 m^2) may not have been sufficiently large to seriously affect the response of the pavement system analyzed. Based on the known effect of changing the average k of the subgrade, it is expected that, as the extent of a weak area of support is increased, it will have increasingly greater impact on the pavement responses.

CONCLUSION

This presentation and discussion show that nonuniform properties of paving materials have a significant effect on the behavioral response of the pavement systems analyzed. Further, the findings suggest that the Monte Carlo simulation may not be the most efficient method for determining the range of pavement responses due to nonuniform material properties. The Monte Carlo simulation technique is valuable in that it permits the calculation of statistical parameters of the pavement response. However, when the Monte Carlo simulation procedure is used, the sample size must be large enough to provide an adequate data base for a reliable statistical analysis of the problem. Results clearly show that a sample size of 10 is inadequate for such an analysis, but the sample size required to obtain a satisfactory simulation was not determined. Probably a combination of the two techniques used in this paper is the most reliable procedure.

It was interesting to note in the findings how the locations of the maximum strains changed with the different sets of randomly assigned properties for the paving materials. These results clearly show why cracks form at different locations in pavement systems even though theoretically the point of maximum stress or strain is at the same location for the different pavements. The phenomenon observed has long been assumed by paving engineers, but, to the authors' knowledge, this is the first time it has been demonstrated with analytical models.

The results clearly show that finite element models can be used to evaluate the effects of nonuniform paving materials on pavement behavior. Much work is still needed, however, to adequately characterize the specific levels of variability in the paving material and the level of nonuniformity that has a critical effect on pavement responses, and the relative severity of the nonuniformity on pavement performance. Such information is needed before models can be developed that will enable the engineer to make realistic trade-offs between better quality control and higher costs.

Work is still needed on the application of these procedures to flexible pavement systems. The problem involves selection of appropriate models and assigning the appropriate values to each element in the model. Associated with assigning of values is the question of the size of an area to represent an appropriate specimen size in the continuum, which will also reflect on the degree of variability in the system.

The procedures presented here can be used to resolve some of these questions, but there is still much work to be done before valid models will be available to make comprehensive risk analyses of pavement designs.

ACKNOWLEDGMENTS

The authors are indebted to the Engineering Experiment Station and the Department of Civil Engineering of the University of Illinois at Urbana-Champaign for their financial and administrative support of this study.

REFERENCES

1. Proceedings, Highway Conference on Research and Development of Quality Control and Acceptance Specifications. U.S. Bureau of Public Roads, Vol. 1, 1965.
2. N. A. Huculak. Evaluation of Pavements to Determine Maintenance Requirements. Highway Research Record 129, 1966, pp. 12-27.
3. CGRA Field Performance Studies of Flexible Pavements in Canada. Proc., Second International Conference on Structural Design of Asphalt Pavements, Ann Arbor, Mich., Aug. 1967.
4. The AASHO Road Test: Report 5—Pavement Research. HRB Special Rept. 61E, 1962.
5. J. R. Levey and E. J. Barenberg. A Procedure for Evaluating Pavements With Nonuniform Paving Materials. Highway Research Record 337, 1970, pp. 55-69.
6. W. R. Hudson and H. Matlock. Analysis of Discontinuous Orthotropic Pavement Slabs Subjected to Combined Loads. Highway Research Record 131, 1966, pp. 1-48.
7. W. R. Hudson and H. Matlock. Cracked Slabs With Non-Uniform Support. Journal ASCE, Vol. 93, No. HW1, 1967.
8. E. L. Wilson. Structural Analysis of Axisymmetric Solids. Journal of American Institute of Aeronautics and Astronautics, Vol. 3, No. 12, 1965.
9. A. C. Eberhardt. Aircraft-Pavement Interaction Studies, Phase 1: A Finite Element Model of a Jointed Concrete Pavement on a Non-Linear Viscous Subgrade. U.S. Army Construction Engineering Research Laboratory, Champaign, Ill., Rept. S-19, 1973.
10. J. R. Levey. A Method for Determining the Effects of Random Variations in Material Properties on the Behavior of Layered Systems. Univ. of Illinois, PhD thesis, 1968.

APPLICATION OF STATISTICAL METHODS TO THE DESIGN OF PAVEMENT SYSTEMS

Michael I. Darter, University of Illinois at Urbana-Champaign

This paper describes some of the applications of statistical or probabilistic methods to the design and analysis of pavement structures and discusses the theory on which they are founded. The major purpose for applying probabilistic methods to design of pavement systems is to help the engineer optimize design. The technology of statistical or probabilistic methods enables the engineer to directly consider the effect of many of the variabilities and uncertainties associated with the design, construction, and in-service life of pavements in the design process. Design adequacy or reliability or, conversely, the probability of distress can therefore be assessed to a much greater degree than without these concepts, and hence more optimal designs can be provided. Basic variabilities and uncertainties involved in the design, construction, and in-service life of pavements are described and shown to have significant effects on performance. Theory to estimate the probable fracture distress and the loss of serviceability of portland cement and concrete pavement due to repeated traffic loadings is presented and illustrated. A relationship between estimated probability of traffic-associated fracture distress and measured slab cracking is developed. The application of these techniques to design is illustrated by several examples. Some of the methods described have been implemented and have been shown to be practical and useful.

•APPLICATION of statistical or probabilistic methods to the design and rehabilitation of pavement systems is an essential step toward improving existing empirical procedures and developing mechanistic procedures. The purposes of this paper are to (a) describe why application of probabilistic methods is important and necessary, (b) outline the methodology for practical and useful application, and (c) provide example applications.

Probabilistic methods have been used extensively for several years in various areas such as structural engineering. The consideration of material variations, traffic load uncertainties, and reliability of a pavement structure was strongly advocated by participants at the FHWA-HRB Workshop on the Structural Design of Asphalt Concrete Pavement Systems in 1970 (1), and this need was listed as one of the 10 most pressing problems facing pavement engineers. Since the workshop, probabilistic methods have been applied to rigid pavement design and analysis by Kher and Darter (2), Darter (3), and Levey and Barenberg (4). Applications to flexible pavements were made by Darter and others (5, 6, 7), Moavenzadeh and others (8, 9, 10), and McManus and Barenberg (11). These efforts provided some significant results, but they represent only a beginning.

This paper discusses the basis for using probabilistic methods in design and rehabilitation and develops the theory and concepts for probabilistic stress-strength, fatigue, and serviceability applications to design and analysis of pavement systems.

BASIS FOR PROBABILISTIC DESIGN

Variabilities and Uncertainties

To those who have been closely associated with design, construction, and subsequent performance of pavements, the words variability and uncertainty have much significance. During design the engineer must estimate many input values from information that is usually very limited; available design procedures are in many respects inadequate. Many material property variations can be observed during construction, and construction deficiencies are also rather common. During the life of the pavement, many performance variations occur that are related to traffic loadings, climatic effects, maintenance procedures, and occurrence of distress along the pavement.

However, if these uncertainties and variations are identified and their magnitude is approximately quantified, they can be used in the design process to achieve more optimum designs. Many of the variabilities have been reported in the literature and therefore will not be repeated here (5, 13). Variations can be conveniently divided into three basic types: variability within a project, variability between assumed and actual design values, and variability due to the inadequacy of the design procedure to account for all necessary factors or to adjust for each factor in the correct manner.

Variation Within a Project

Factors that often vary within a construction project include aggregate gradation, thickness, moisture content, density, resilience, and strength. For example, strength variations in portland cement concrete (PCC) occur from point to point along a pavement slab and are caused by many factors including batching, mixing, transporting, placing, finishing, and curing. A frequency distribution of compressive core strength determined at 500-ft (150-m) intervals along one project is shown in Figure 1. A core thickness frequency distribution from the same project is shown in Figure 2. These are typical distributions, but some projects show much greater variability, particularly where inadequate concrete consolidation has occurred.

Variations in Assumed and Actual Design Values

Actual values often vary considerably from those predicted in the design phase. Factors that vary include actual versus design material resiliency and strength, actual versus predicted traffic loadings, and even actual versus predicted climatic conditions. Perhaps the most obviously uncertain design factor that must be estimated is the traffic loadings expected over the life of the pavement. Social, economic, and political factors cause much uncertainty in traffic forecasting. Probably the most dramatic difference between estimated and actual traffic has occurred for high-volume freeways. Pavement design for the New Jersey Turnpike was based on an estimate of 20 million vehicle applications, but actual 20-year counts showed more than 90 million applications. Similar situations have occurred on other highways such as the Dan Ryan Expressway in Chicago (26). Deacon and Lynch (14) estimated equivalent wheel loads for 20 locations in Kentucky by using a new method and compared the predictions with actual data measured over about 20 years. They concluded that the actual traffic will usually fall between one-half and twice the best estimate.

Variation Due to Inadequacy of Design Procedure

An interesting example of the inadequacy of design procedures can be obtained from the results of the AASHO Road Test for flexible or rigid pavements. The number of load applications to a terminal serviceability index of 2.0 was computed for several flexible sections by using the design equations developed at the road test and included in the AASHO Interim Guide (15). The computed load applications were then plotted versus the actual load applications (Figure 3) for flexible pavements. The scatter of data is indicative of the inability to predict performance with these empirical equations even under controlled testing conditions. To this uncertainty must be added uncertainties that are imposed when the design equations are used in other climates and soils and for mixed traffic loadings.

Statistical Analysis Units

As a pavement is subjected to traffic and environmental effects, various types of distress occur at seemingly random locations along the pavement. The variation along the project must be carefully estimated for the probabilistic approach to be meaningful. It is helpful to the analysis to consider the pavement as a series of short lengths or areas within which pavement properties are assumed to be homogeneous and the variability along the project is considered to be between these pavement lengths or areas. The size of these so-called statistical analysis units can vary depending on the purpose of the analysis from say 1-ft^2 (0.09-m^2) areas to 200-ft (61-m) pavement lengths. The smaller the area is, the greater the variability of mean values is, however.

Design Goal: Optimization

Choosing the best possible design for a given project situation, or optimizing, is a subject of vital importance to the pavement engineer and the essence of modern engineering practice. The increased need for better optimization arises from the scarcity of pavement funds, materials, and fuel on one hand and increasing public demand for better pavement performance and less traffic delay due to excessive maintenance activities on the other hand.

Probabilistic design applications help the engineer to achieve greater optimization in design in several ways. First, they permit direct consideration of variations and uncertainties. The applied safety factors are direct functions of the existing variations and uncertainties and, hence, increase or decrease depending on the amount of variations and uncertainties.

Second, probabilistic design procedures enable the engineer to predict occurrence of random distress. The amount of distress is directly related to the amount of required maintenance, which on pavements that carry moderate to high traffic volumes has significant effects on user delays.

Third, such design procedures provide the technology so that the engineer can better assess the reliability of designs and design pavements with different traffic volumes or functional requirements at different levels of reliability (e.g., farm-to-market road versus high-volume freeway).

Finally, use of the procedures optimizes facility and user costs. By designing pavements at the level of reliability best suited for each situation, the engineer minimizes total life cycle costs (including initial construction, maintenance, overlay, and user delay costs). This is particularly important, for example, for high-volume pavements where the consequence of failure is severe user delay due to required maintenance activities (12).

PROBABILISTIC STRESS-STRENGTH ANALYSIS AND DESIGN

Whenever the stress level in any portion of a pavement structure exceeds strength, a fracture occurs. The probability of fracture can be defined as

$$p_f = P(S > F) \qquad (1)$$

where

P = probability of occurrence,

S = applied stress, and
F = strength.

Conversely the probability of no fracture, or the reliability R, can be defined as R = 1 - p_f. The magnitude of strength within a pavement structure is a random variable in that it varies from point to point. The magnitude of applied stress is also a random variable that depends in part on loading conditions from both climate (temperature and moisture) and traffic. Because both stress and strength are random variables, p_f can be expressed as

$$p_f = P(S > F) = P(d > 0) \tag{2}$$

where d = F - S. Therefore, f(d) is the difference density function of S and F. It is reasonable to assume, based on limited data, that the stress magnitude from heavy cargo vehicle loadings is approximately normally distributed (25); it has been fairly well established that the strength of many materials is approximately normally distributed. Because the level of p_f is relatively large for pavements, the effect of the exact shape of the distribution curve in the tail portion is less, and the assumption of normality appears reasonable. If F and S are normally distributed, d will also be normally distributed (Figure 4).

Bars are used above the expressions to represent their mean values:

$$\bar{d} = \bar{F} - \bar{S} \tag{3}$$

The standard deviation of d σ_d can be computed as follows:

$$\sigma_d = \sqrt{\sigma_S^2 + \sigma_F^2} \tag{4}$$

As shown in Figure 4, the probability of fracture p_f is given by the area to the left of 0.

$$p_f = P(d < 0) = P(-\infty < d < 0) = \int_{-\infty}^{0} f(d)\,d(d) \tag{5}$$

Reliability is the area to the right of 0 as shown.

Normal distribution tables can be used to calculate p_f or R. For example, consider a 7-in. (180-mm) PCC slab under a 9,000-lbf (40-kN) wheel load located at its edge. The mean tensile stress at the critical location in slab (based on Westergaard's edge equation) is $\bar{S}$ = 360 psi (2500 kPa). The mean flexural strength of the slab is $\bar{F}$ = 690 psi (4760 kPa).

$$\sigma_S = 48$$

$$\sigma_F = 104$$

Therefore,

$$d = 690 - 360 = 330$$

$$\sigma_d = \sqrt{48^2 + 104^2} = 115$$

The parameter d must now be transformed into a normal variate with a mean of zero and variance of one so that normal distribution tables can be used.

$$Z = \frac{d - \bar{d}}{\sigma_d} = \frac{0 - \bar{d}}{\sigma_d} = \frac{-330}{115} = -2.87$$

The area under the normal curve from $-\infty$ to -2.87 is 0.0021; therefore, $p_f = 0.21$ percent. An illustration of this area of failure is shown in Figure 5 where the actual distributions of the flexural strength and stress for a 7-in. (180-mm) slab are shown to overlap. This area of overlap is not the probability of failure but a function of the probability of failure. The figure also shows the stress distribution for a 9-in. (230-mm) slab where the probability of failure is very small. The other design inputs for this pavement section are given in Table 1.

In engineering terms, the probability of fracture in the PCC slab is 0.21 percent, or, given the large number of these slabs that would exist along a pavement project, about 0.21 percent of these 7-in. (180-mm) slabs would be expected to fracture if this stress level is applied to all. Note that fracture is, at most, only an initial hairline crack at the critical point in the slab. It is well-established that collapse load is at least twice the load calculated by the Westergaard expression. However, only a few load applications will cause the crack to widen and perhaps result in a serious failure condition as observed on in-service pavements and at the AASHO Road Test. The basic assumptions made in this analysis are that (a) stress and strength are normally distributed and (b) they are independent random variables.

Determination of the variations (or standard deviations) of S and F in real pavement structures is the next task. Again the example of a PCC pavement slab will be used for illustration. Stress is a function of several variables:

$$S = f(E, t, k, P, \ldots) \qquad (6)$$

where

E = concrete modulus of elasticity,
t = slab thickness,
k = modulus of foundation support, and
P = traffic wheel load.

The flexural strength of the concrete is also a function of several parameters:

$$F = f(M, C, Q, \ldots) \qquad (7)$$

where

M = materials used (quantity and type),
C = curing, and
Q = consolidation.

Figure 1. Variation of compressive strength of cores cut in 500-ft (150-m) intervals from a PCC slab.

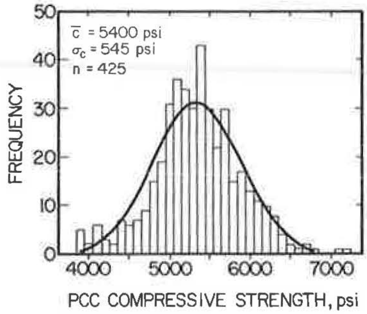

Figure 2. Variation of PCC slab thickness.

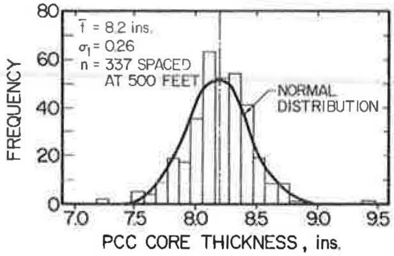

Figure 3. Actual versus predicted 18-kip (80-kN) single-axle load applications.

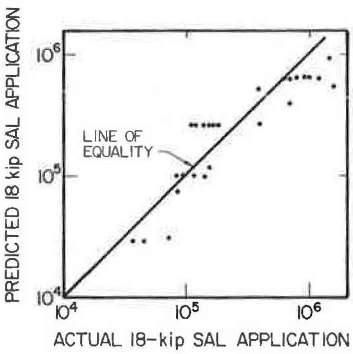

Figure 4. Distribution of d = F - S showing areas of failure probability and reliability.

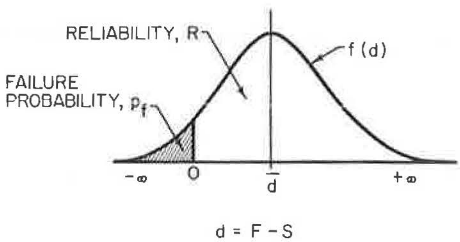

Figure 5. Distribution of flexural strength along a PCC slab and distributions of applied stresses estimated by using Westergaard's edge loading model.

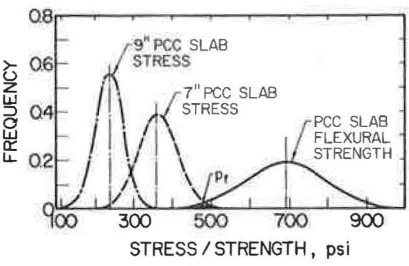

Table 1. Description of design inputs for a jointed PCC pavement.

		Expected Variation (percent)		
Design Factor	Mean	Low	Medium	High
Flexural strength, psi	690[a]	10	15	25[b]
Modulus of elasticity, psi	4.2×10^6	10	15	25[b]
Modulus of foundation support (top of subbase), lbf/in.^{3}				
k_c	108	20	35	50[b]
k_s	61			
Initial serviceability	4.5	—[c]		
Terminal serviceability	2.5			
Forecast 20-year 18-kip EAL in design lane	5×10^6			
Design equation variance of log W (error)	0		0.0353[d]	
Slab thickness, in.	Varies	—[e]		

Note: 1 psi = 6.9 kPa; 1 lbf/in.^{3} = 271 kN/m^3; 1 kip = 4.4 kN; 1 in. = 2.5 cm.

[a]Third point loading, 28-day curing.

[b]Coefficient of variation.

[c]Expected variation of 0.2 (low), 0.3 (medium), and 0.4 (standard deviation).

[d]Estimated from AASHO data (2).

[e]Expected variation of 0.2 (low), 0.3 (medium), and 0.5 (standard deviation).

The variation in S and F will, of course, depend on the variability of the factors that influence them. A linear first-order approximation may be used to determine the variance of S, for example, as a function of variations of the parameters E, t, k, and P according to the Westergaard stress model. This variance equation for S can be derived by using a Taylor's Series expansion of the function about its mean (5). The resulting expression, if we neglect moments greater than second order, is as follows assuming independence of the factors (for stress):

$$\sigma_S^2 \simeq \sum_{i=1}^{j} \left(\frac{\partial S}{\partial X_i}\right)^2 \sigma_{X_i}^2 \tag{8}$$

where

σ_S^2 = variance of S,
X_i = random variables included as parameters in S (i.e., E, t, k, P), and
$\sigma_{X_i}^2$ = variance of X_i.

The variance of S can then be determined as a function of the variations of E, t, k, P, and e, which is a random variable representing the inadequacies of the Westergaard equation to predict the true tensile stress in the slab.

$$\sigma_S^2 \simeq \left(\frac{\partial S}{\partial E}\right)^2 \sigma_E^2 + \left(\frac{\partial S}{\partial t}\right)^2 \sigma_t^2 + \left(\frac{\partial S}{\partial k}\right)^2 \sigma_k^2 + \left(\frac{\partial S}{\partial P}\right)^2 \sigma_P^2 + \sigma_e^2 \tag{9}$$

Equation 9 is called the variance equation of S and is given in full elsewhere (3). This technique has been used on several design models (2, 5, 7) and has compared well to simulation results (<±10 percent).

Determination of σ_E, σ_k, . . . , is an important task that requires special consideration. For example, consider the selection of the standard deviation of the foundation support modulus k. This parameter will vary from point to point along the grade. Predicting its mean value during the service life of the pavement will also be uncertain because of pumping and settlement conditions, and it will vary through the year depending on factors such as moisture and temperature. These variabilities can be estimated from past construction and performance data, if available, or from direct testing or experience, if necessary. These sources of variability must finally be combined to give an overall σ_k for use in design.

An application of these stress-strength concepts is presented by showing the effects of overloads on distress occurrence. Overloads in this example are considered as single-axle loads greater than 18 kips (80 kN). Again, the variations of material properties, thicknesses, and loads can be estimated, and the resulting variations in stress along the pavement can be predicted by using Westergaard's edge loading model (21) according to variance equation 9. In this example, the Westergaard edge loading model was selected and a variance expression was derived (3). The probability that tensile stress would exceed strength was calculated according to equation 5 for a 9-in. (230-mm) slab thickness. A plot of p_f versus axle load is shown in Figure 6. The upper curve represents a situation where material properties, thicknesses, and the like vary considerably along a project. The lower curve represents more uniform conditions (or better quality control) as given in Table 1. The type of fracture considered here is definitely not collapse fracture as discussed but is at most initial hairline cracking, which usually leads rapidly to wider cracks.

Results shown in Figure 6 indicate the relative effect of overloads on distress occurrence. For example, for an axle load of 24 kips (107 kN), the proportion of cracking as the load rolls along the pavement edge would vary from 0.03 to 1.8 percent compared to 0.002 to 0.49 percent for an 18-kip (80-kN) single-axle load. The effect of variations on distress is very evident from these analyses.

PROBABILISTIC FATIGUE ANALYSIS AND DESIGN

Fatigue Analysis

Repeated load applications cause several types of damage to pavement structures including fracture, permanent deformation or distortion, and disintegration. Basic theory is presented for damage due to fracture, but probabilistic concepts can also be extended to other distress types.

The basic approach shown in Figure 7 will be developed by using the PCC slab example previously described. First, the mean stress and its variation must be estimated from the means and variances of the parameters on which it depends as previously described (Figure 5). The mean strength $\bar{F}$ and standard deviation σ_F must also be estimated. Next a fracture fatigue curve must be obtained for the material under consideration such as the following for plain PCC (16):

$$\log_{10} N_{f_i} = a + b\left(\frac{S_i}{F}\right) \tag{10}$$

where

- N_{f_i} = load applications to fracture of a specimen in bending at i th load level,
- a = 19.3,
- b = -20.2, and
- S_i = concrete tensile stress at critical location in slab due to i th load.

The variation of N_f will be a function of the variation of S, F, and other unknown parameters denoted by e′. A variance expression can be derived as follows:

$$\sigma^2_{\log N_f} \simeq \left(\frac{\partial \log N}{\partial S}\right)^2 \sigma_S^2 + \left(\frac{\partial \log N}{\partial F}\right)^2 \sigma_F^2 + \sigma_{e'}^2 \tag{11}$$

A fatigue damage model must now be used to determine the effect on accumulated damage of varying wheel load magnitude. Miner's damage expression has been used in previous design and will be used here:

$$D = \sum_{i=1}^{m} \frac{n_i}{N_i} \tag{12}$$

where

- D = total accumulated fatigue damage over pavement design life,
- n_i = number of applied loads of i th magnitude, and
- N_i = number of allowable traffic loads of i th magnitude at fracture.

D is not a constant for a pavement but varies depending on the randomness of n_i and N_i. There is a significant uncertainty in predicting n_i and variability in N_i. There are some data and theory to support the assumption that these variables are approximately lognormally distributed (5). Inasmuch as D is the sum of one or more ratios of n to N, its distribution will depend on the distribution of n and N. As a first-order approximation, it is assumed that D follows a lognormal distribution since both n and N are approximately lognormally distributed. Even though the quotient of two normally distributed random variables does not exactly follow a normal distribution, simulation and theory show that it is practically normally distributed. The total variation in D can be determined as

$$\sigma_D^2 \simeq \sum_{i=1}^{m} \left(\frac{\partial D}{\partial N_i}\right)^2 \sigma_{N_i}^2 + \sum_{i=1}^{m} \left(\frac{\partial D}{\partial n_i}\right)^2 \sigma_{n_i}^2 \qquad (13)$$

where

σ_D^2 = variance of accumulated damage,
$\sigma_{N_i}^2$ = variance in allowable fatigue applications to fracture (can be estimated from equation 11), and
$\sigma_{n_i}^2$ = variance in forecast traffic applications (5).

Finally, the distribution of fatigue damage D along a pavement can be obtained as shown in Figure 7. The probability of fatigue fracture p_{ff} is

$$p_{ff} = P(D > 1.0) = P(\log_{10} D > 0) \qquad (14)$$

If we assume that D is lognormally distributed, p_{ff} can be readily calculated as previously described. p_{ff} represents the probability that a slab will fracture because of fatigue, or for a long section of pavement it represents a proportion of length or area along the pavement that will fracture or crack because of traffic load bending stresses. Its relation to the cracking index will be discussed subsequently.

Example of Fatigue Damage Application

The theory and concepts for applying probabilistic methods to fatigue damage have been presented. This application is significant in interpreting the extent of fracture that may occur if a pavement is designed for $\bar{D}$ = 1.0, as is the usual case. The deterministic approach leaves much to be desired in that no assessment of how much cracking will occur when D = 1.0 can be made.

This example uses AASHO Road Test rigid pavement data and a probabilistic distress analysis to show the correlation between the possibility of distress and the cracking index or linear feet of slab cracking per 1,000 ft^2 (93 m^2) of pavement. The procedure shown in Figure 7 is followed in the analysis of the various road test slabs.

1. Means and standard deviations of the pavement factors E, k, t, and P were determined from road test data (20), for all pavement sections that were subjected to single-axle loadings ranging from 3.5 to 9.5 in. (89 to 241 mm) in slab thickness for both reinforced and nonreinforced sections. For example, for section 523, loop 5, reinforced slab,

Factor	Value	Coefficient of Variation
$\bar{t}$, in.	6.5	0.05
$\bar{E}$, psi	6.25×10^6	0.15
$\bar{P}$, kips	11.2	0.10
$\bar{F}$, psi	790	
$\bar{k}$, lb/in.^{3}	108	0.35

In this example, $\bar{F}$ has a standard deviation of 61 psi (421 kPa). [k determined for loss of support of this slab due to severe pumping is 9 lbf/in.^{3} (2.4 MN/m^3).]

2. The Westergaard interior load stress model (21) is used to predict the mean maximum tensile stress of PCC slabs. Through use of the finite element program and the measured AASHO Road Test stresses, it is found that the Westergaard interior load model predicted reasonable maximum stresses that would occur from a load located about 20 in. (508 mm) from the pavement edge, which is the approximate mean of the outside wheel path loads at the road test. The loss of support for each slab due to pumping is considered through a reduction in the k-value by means of the correlation developed by McCullough and Yimpasert (22) between pumping index and eroded area and the correlation developed by Kher et al. (18) between eroded area and modified k-value. When pumping occurred, the modified k-value is used in the Westergaard interior stress calculation. The thermal shrinkage stress of the slabs is also considered by assuming an average temperature differential of 1 deg F/in. (0.219 deg C/cm) of slab throughout the loading period and by using the interior warping stress model developed by Westergaard (23) and Bradbury (24). Hence, the final stresses used in the fatigue damage analysis considered slab loss of support from pumping and a small thermal tensile warping stress.

As previously discussed, a variance equation was developed from the Westergaard interior stress model by using equation 9 so that the variation in stress due to variations in the design parameters E, k, t, and P could be estimated. For example,

$\bar{S}_{traffic}$ = 443 psi (3054 kPa), standard deviation = 60 psi (414 kPa);
$\bar{S}_{temp\,warp}$ = 82 psi (565 kPa), 40-ft (12-m) joint spacing; and
$\bar{S}_{tot}$ = 525 psi (3620 kPa), critical tensile stress for interior loading.

3. The fatigue S-F:N curve determined by Kesler (16) for plain dry portland cement concrete is used as defined by equation 10. The variance of this equation as derived by equation 11 is

$$\sigma^2_{\log N_f} \simeq \frac{408\sigma_S^2}{F^2} + \frac{408\bar{S}^2\sigma_F^2}{F^4} \qquad (15)$$

For example,

$\log \bar{N}_f = 19.3 - 20.2\,(S/F) = 5.8759$, or $\bar{N}_f$ = 751,450 load applications; and
$\sigma_{\log N_f} = 1.8514$ (from equation 15).

4. Miner's damage hypothesis is used to predict the average amount of fatigue damage for the AASHO Road Test slab and loading combination. The variance of D for each slab is computed by using equation 13, and the probability of distress is calculated according to equation 14.

$$\bar{D} = \sum \frac{n_1}{N_1} = \frac{828{,}000}{751{,}450} = 1.102$$

or

$$\log \bar{D} = 0.0421$$

$$\sigma_D^2 \simeq \frac{\sigma_{n_1}^2}{N_1^2} + \frac{N_1^2}{N_1^4}\sigma_{n_1}^2 = 22.06$$

where

$\sigma_{n_1}^2$ = 0 (i.e., no error in determining load applications applied at the road test),
N_1 = 751,450 load applications,
n_1 = 828,000 load applications to serviceability index of 2.5 (20), and
$\sigma_{N_1}^2 \simeq \frac{\sigma_{\log N} \bar{N}_1^2}{0.1886}$.

Therefore,

$$\sigma_{\log D} \simeq \frac{(0.4343)\,\sigma_D}{\bar{D}} = 1.8514$$

The probability of distress is estimated from the distribution of log D as follows:

$$z = \frac{0.0 - 0.0421}{1.8514} = -0.023$$

From normal distribution tables, the area from -0.023 to $+\infty$ is the probability of distress, which equals 0.51 or 51 percent.

5. The cracking index is determined for each slab, either at a serviceability index of 2.5 or at termination of the test at n = 1,114,000 load applications. The cracking index for this example section is 121 ft/1,000 ft^2 (403 m/1000 m^2), which corresponds to a probability of distress of 51 percent. A plot of probability of distress [or $P(D > 1)$] versus cracking index for the nonreinforced slabs is shown in Figure 8 and for reinforced slabs in Figure 9. A fair correlation exists but there is much scatter. For example, at a probability of distress of 50 percent, or when $\bar{D} = 1$, the cracking index is about 90 ft of cracking per 1,000 ft^2 (333 m/1000 m^2) for the nonreinforced slabs or an average of about 16 linear ft (4.9 m) of cracking per 15-ft (4.6-m) slab. This amount of cracking would have a significant effect on serviceability rating and also on maintenance requirements of the pavement. A cracking index of 90 would correspond to a serviceability rating of about 1.5 to 2.2 according to Figure 17-F in the road test report (20). From Figure 17-F in the AASHO Road Test report and Figure 9, a probability of fatigue fracture of 50 percent or $\bar{D} = 1$ corresponds to a terminal serviceability of approximately 1.5 for reinforced slabs. Therefore, it seems that, for the road test pavements at least, designing at $\bar{D} = 1$ may produce a pavement that will show extensive cracking before the design number of load applications is applied.

This probabilistic fatigue damage approach is of course simplified in several respects but has definite advantage for use in design over the deterministic approach. A plot of probability of distress versus slab thickness for given pavement design situations

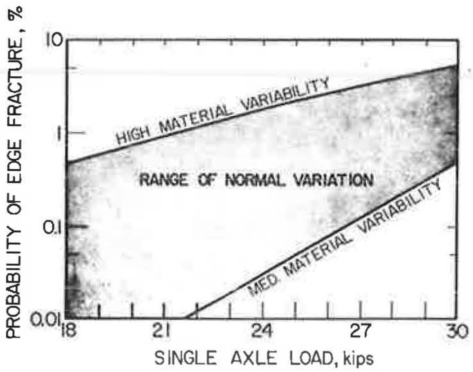

Figure 6. Estimated probability of edge fracture versus mean single-axle load for a 9-in. (230-mm) PCC slab.

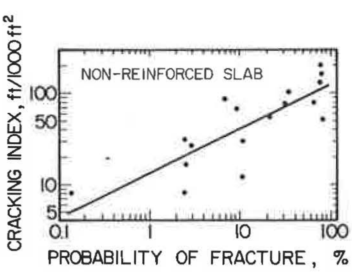

Figure 8. Cracking index versus estimated probability of fracture for AASHO Road Test nonreinforced rigid pavement sections.

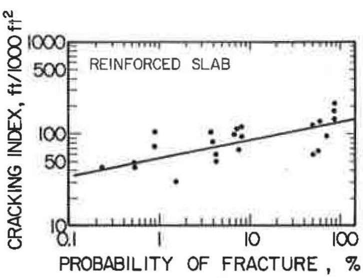

Figure 9. Cracking index versus estimated probability of fracture for AASHO Road Test reinforced rigid pavement sections.

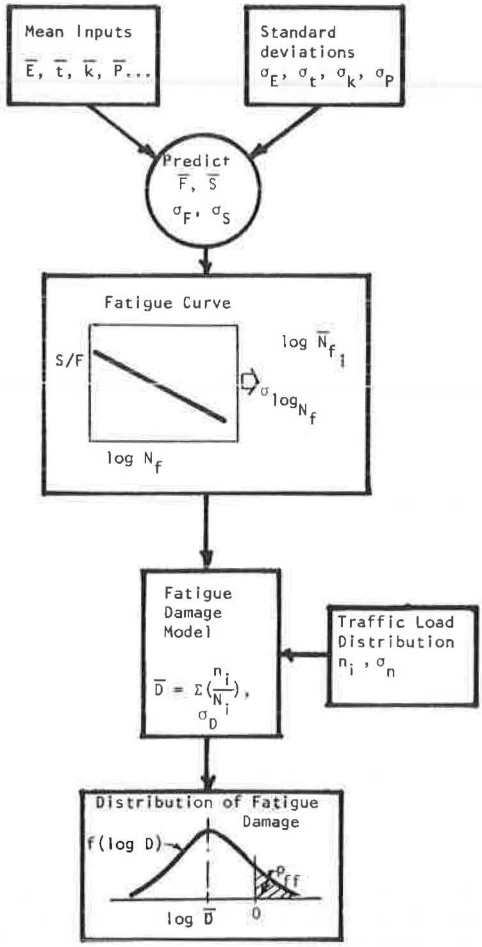

Figure 7. Approach for determining probability of fracture distress due to repeated traffic loadings.

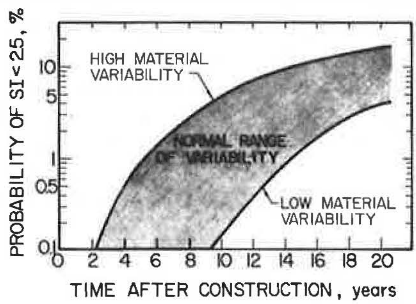

Figure 10. Years since construction versus estimated probability of the serviceability index being less than 2.5.

can be determined to assist in selecting the final design thickness. An estimate of the extent of cracking also provides information about the required maintenance.

PROBABILISTIC SERVICEABILITY ANALYSIS AND DESIGN

Serviceability Design Application

Probabilistic serviceability methods have been applied to four existing empirical design methods including the Texas flexible pavement design system (5, 6), the SAMP6 flexible pavement design system (17), AASHO rigid pavement design procedures (2), and the Texas rigid pavement design system (18).

The probability of distress is defined in terms of the probability of the serviceability level of a section of pavement dropping below a minimum acceptable level. If the loss of serviceability is predominantly due to traffic loadings, then

$$p_{sf} = P(w > W) \tag{16}$$

where

p_{sf} = probability that a pavement section will reach a minimum acceptance serviceability level during a specified design period,
w = forecast 18-kip (80-kN) equivalent single-axle load applications over design period, and
W = allowable 18-kip (80-kN) equivalent single-axle load applications at acceptable serviceability level (calculated from a predictive model based on the serviceability-performance concept).

It is important to realize that this definition considers only the detrimental effect of traffic loadings. In areas where much of the loss in serviceability is due to environmental conditions, the equation for W (if based on the AASHO Road Test results) must be modified to account for the additional detrimental effects.

Because the concept and theory concerning probabilistic serviceability analysis and design have been published in the references previously cited, only a few examples illustrating the application will be given.

Rigid Pavement Example

Consider the structural design of the pavement described in Table 1. Structural thickness of the PCC slab can be determined according to a commonly used deterministic design procedure such as AASHO Interim Guide (15). For the given foundation support, traffic, and other factors, jointed concrete slab thickness of 9.0 in. (230 mm) is required. The only applied safety factor is the reduction of working stress to three-fourths of the flexural strength.

An analysis is conducted by using probabilistic methods to analyze the performance and adequacy of this design. The variability of pavement serviceability level along the project as traffic loads are accumulated over time can be predicted by using the variance expression developed by Kher and Darter (2, equation 20). The variation of material properties along the pavement, possible design assumption errors, and design equation inadequacy must be estimated for the project as given in Table 1. If we assume a linear increase in traffic applications, the percentage of pavement area that will reach terminal serviceability at any time can be computed as follows.

The mean $\overline{W}$ for the jointed concrete pavement to reach terminal serviceability is 13.3×10^6 18-kip (80-kN) equivalent axle loads (EALs) based on the AASHO performance equation. The variance of log W due to a high level of variability in material properties, slab thickness, and lack of fit of the model is computed as

$$\sigma^2_{\log W} = 0.202$$

by using Kher and Darter's equation 20 (2). The percentage of pavement to reach terminal serviceability after 3×10^6 18-kip EALs is computed as

$$Z = \frac{\log_{10}(13.3 \times 10^6) - \log_{10}(3 \times 10^6)}{\sqrt{0.202}} = 1.44.$$

From normal distribution tables, the area between $-\infty$ and 1.44 is 0.075; therefore, p_{sf} = 7.5 percent. The 3×10^6 18-kip EALs are accumulated at 12 years assuming a linear increase of traffic with time. A plot of p_{sf} versus time in years since construction is shown in Figure 10. For example, at 10 years, the proportion of the project reaching a minimum acceptable serviceability level may range from about 0.1 to 5 percent, depending on the level of variability. At 20 years, the proportion reaching this level will be from 4 to 17 percent assuming only normal routine maintenance has been applied. How much pavement area can be allowed to reach this state of deterioration before major rehabilitation of the entire pavement is necessary depends on several factors such as traffic volume, available funds, and maintenance policies but may range between 5 to 30 percent.

Based on these examples, it is obvious that the traffic-load-associated distress shown in Figure 10 can be either reduced or increased by varying the thickness of the PCC slab (holding the subbase and subgrade constant) according to the AASHO design models. It is interesting to note that the original AASHO Road Test pavement sections still in service on I-80 in Illinois tend to confirm this conclusion after 16 years of service. There is less distress in the 11- and 12.5-in. (279- and 318-mm) reinforced slab sections than in the 8- and 9.5-in. (203- and 241-mm) sections. Hence, slab thicknesses that provide varying levels of traffic load design reliability can be determined. If environmental deterioration has a significant effect, the calculated reliability will be greater than the actual reliability. Also if other factors such as the slab joints show serious distress (i.e., poor joint design), the actual reliability will be less than the calculated reliability. Either the variance equation derived from the AASHO equations can be used directly or a nomograph developed by Kher and Darter (2) can be used to determine slab thickness at varying levels of R as shown in Figure 11.

Flexible Pavement Example

Similar examples can be developed for flexible pavements. The Texas flexible pavement system (FPS) considers variability in several parameters. The design system can provide designs at various levels of design reliability for traffic-related distress including complete life cycle costs. A summary of six pavement designs ranging in reliability from 50 to 99.99 percent is given in Table 2 for a recently constructed high-volume urban freeway.

The selection of the level of design reliability is an important task. An approximate estimate of the minimum level of reliability using the Texas FPS for various types of projects ranging from farm-to-market roads to urban freeways was determined based on the judgment of experienced pavement engineers. The selected design reliability increases with the function or type of highway pavement being designed, its urban or rural location, and the traffic volumes and equivalent load applications expected (5, 12, 19). Again, these reliability levels should not be considered as absolute values inasmuch as they are relative to the accuracy of the estimated variations of the design parameters and adequacy of the design equation.

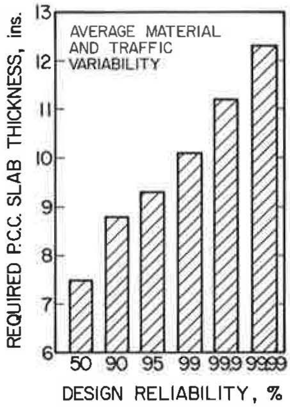

Figure 11. Design reliability (for traffic loadings) versus required PCC slab thickness for a given subbase and subgrade.

Table 2. Summary of optimum (total costs) designs for flexible pavement at various levels of reliability.

	Reliability Level (percent)					
Design Criteria	50	80	95	99	99.9	99.99
Initial cost	2.66	3.20	3.68	3.73	4.41	5.19
Routine maintenance	0.28	0.28	0.28	0.23	0.22	0.22
Overlay	0.00	0.00	0.00	0.27	0.54	0.50
User delay	0.00	0.00	0.00	0.29	0.16	0.24
Salvage	-0.32	-0.39	-0.49	-0.55	-0.69	-0.77
Total, $/SY	2.62	3.09	3.47	3.97	4.64	5.38
Thickness, in.						
Asphalt concrete	2.00	2.25	2.00	2.00	2.00	2.00
Black base	2.75	3.25	3.50	3.00	3.50	5.55
Crushed stone	6.00	8.00	12.00	14.00	18.00	18.00
Initial life, years	21.6	21.4	21.0	10.5	9.2	9.5
Overlay thickness, in.				1.3	2.3	2.3
Life of overlay, years				20.0	22.0	22.0

Note: 1 in. = 2.5 cm.

SUMMARY

Applying statistics or probabilistic methods to the design and analysis of pavements provides the technology for important applications not possible before. These include the following:

1. Provides the basis from which design optimization can be conducted—the degree of design adequacy can be balanced between facility costs and pavement user costs and effects;
2. Makes the design process sensitive and capable of adjusting for many of the uncertainties and variabilities associated with pavement design, construction, and performance;
3. Enables estimation of the amount of distress occurring along a pavement—reasonable correlation was found, for example, between the probability of fatigue fracture distress and cracking index for rigid pavements (the methodology may ultimately lead to prediction of maintenance requirements); and
4. Provides the capability to design at various levels of reliability—therefore, design adequacy can be estimated much better than ever before.

ACKNOWLEDGMENTS

This study was conducted at the Transportation Research Laboratory, University of Illinois. The author wishes to thank Stephen Alfield and Paul McNabb for their assistance with the analysis.

REFERENCES

1. Advisory Committee. Summary of Research Needs. HRB Special Rept. 126, 1971, p. 8.
2. R. K. Kher and M. I. Darter. Probabilistic Concepts and Their Applications to AASHO Interim Guide for Design of Rigid Pavements. Highway Research Record 466, 1973.
3. M. I. Darter. Probabilistic Applications to Rigid Pavement Structures. Presented at the ASCE Specialty Conference on Probabilistic Methods in Engineering, June 24-26, 1974, Stanford Univ.
4. J. R. Levey and E. J. Barenberg. A Procedure for Evaluating Pavements With Nonuniform Paving Materials. Highway Research Record 337, 1970.
5. M. I. Darter and W. R. Hudson. Probabilistic Design Concepts Applied to Flexible Pavement Design System. Texas Highway Department; Texas Transportation Institute, Texas A&M Univ.; and Center for Highway Research, Univ. of Texas at Austin, Research Rept. 123-18, May 1973.
6. M. I. Darter, W. R. Hudson, and J. L. Brown. Statistical Variation of Flexible Pavement Properties and Their Consideration in Design. Proc., AAPT, Vol. 42, 1973, pp. 589-615.
7. M. I. Darter, B. F. McCullough, and J. L. Brown. Reliability Concepts Applied to the Texas Flexible Pavement System. Highway Research Record 407, 1972, pp. 146-161.
8. F. Moavenzadeh. Damage and Distress in Highway Pavements. HRB Special Rept. 126, 1971, pp. 114-139.
9. H. Findakly, F. Moavenzadeh, and J. Soussou. Stochastic Model of Pavement Systems. Transportation Engineering Journal, Proc., ASCE, Vol. 100, No. TE1, Feb. 1972, pp. 57-70.
10. J. E. Soussou, F. Moavenzadeh, and H. K. Findakly. Synthesis for Rational Design of Flexible Pavements: Parts I and II. M.I.T., 1973.
11. P. F. McManus and E. J. Barenberg. Impact of Subgrade Variability on Pavement Construction-Maintenance Cost Trade-Offs. TRB Special Rept. 148, 1974.
12. M. I. Darter, W. R. Hudson, and R. C. G. Haas. Selection of Optimal Pavement Designs Considering Reliability, Performance, and Costs. Transportation Research Record 485, 1974, pp. 67-79.
13. G. B. Sherman. In Situ Materials Variability. HRB Special Rept. 126, 1971, pp. 180-190.
14. J. A. Deacon and R. L. Lynch. Determination of Traffic Parameters for the Prediction, Projection, and Computation of EWL's. Kentucky Highway Department, Final Rept. KYHPR-64-21, 1968.
15. AASHO Interim Guide for Design of Pavement Structures. American Association of State Highway Officials, 1972.
16. C. E. Kesler. Effect of Speed of Testing on Flexural Fatigue Strength of Plain Concrete. HRB Proc., Vol. 32, 1953, pp. 251-258.
17. R. L. Lytton, W. F. McFarland, and D. L. Schafer. Flexible Pavement Design and Management—Systems Approach Implementation. NCHRP Rept. 160, 1975.
18. R. K. Kher, W. R. Hudson, and B. F. McCullough. A Systems Analysis of Rigid Pavement Design. Center for Highway Research, Univ. of Texas at Austin, Research Rept. 123-5, 1971.
19. Flexible Pavement Designer's Manual: Part I—Texas Highway Department Pavement Design System. Highway Design Division, Texas Highway Department, 1972.
20. AASHO Road Test: Report 5—Pavement Research. HRB Special Rept. 61E, 1962.
21. H. M. Westergaard. Stresses in Concrete Pavements Computed by Theoretical Analysis. Public Roads, Vol. 7, No. 2, 1926.
22. P. Yimpasert and B. F. McCullough. Fatigue and Stress Analysis Concepts for Modifying the Rigid Pavement Design System. Texas Highway Department, Research Rept. 123-16, 1973.
23. H. M. Westergaard. Analysis of Stresses in Concrete Pavements Due to Variations of Temperature. HRB Proc., 1926.

24. R. D. Bradbury. Reinforced Concrete Pavements. Wire Reinforcement Institute, Washington, D.C., 1938.
25. J. L. Buffington, D. L. Schafer, and W. G. Adkins. Procedures for Estimating the Total Load Experience of a Highway as Contributed by Cargo Vehicles. Texas Transportation Institute, Texas A&M Univ., Research Rept. 131-2F, 1970.
26. Unexpected Traffic Volume Cuts Pavement Life. Engineering News-Record, Vol. 18B, No. 20, May 20, 1971, p. 25.

STOCHASTIC MODEL FOR PREDICTION OF PAVEMENT PERFORMANCE

Fred Moavenzadeh, Massachusetts Institute of Technology

A simulation model for predicting the performance of highway pavement is described. The primary modes of distress considered are deformation and cracking. The factors contributing to pavement distress are divided into three categories: (a) physical properties and pavement geometry, (b) vehicular load, and (c) environmental conditions. The damage formulation is handled in two steps. The first step yields the stress and strain fields within the system, which are then used as inputs to the second step. The second step yields damage components or limiting responses. Based on the expected values of the damage component, the road serviceability load after a given time period can be predicted by using a relationship similar to that of AASHO serviceability. The model, then, estimates the change in serviceability and associated reliability of the system due to accumulation of damage. After the changes in serviceability and reliability are determined, several possible maintenance strategies can be examined. An essential part of the model is a relationship among maintenance, change in reliability, and the increase in expected life. Thus for each maintenance strategy there is an associated reliability-life expectancy.

•RATIONAL analysis and design of highway pavements, as with any other engineering system, are normally facilitated by the development of models representative of system behavior under realistic operating conditions. A model, in this context, is an abstract representation of the form, function, and operation of the real or physical system. To develop such models requires that the system be characterized realistically and that information about the system's functions, behavioral interactions, and failure patterns and mechanisms be identified. A major task in this development is choosing the proper model. Different analysts may formulate different models for the same system. This difference may be caused by differences either in formalism or in abstraction. It is also possible that this subjectivity and arbitrariness in problem definitions may result in nonunique solutions for such problems. Consequently, decisions on the configuration and structure of models to represent certain problems may vary considerably among analysts, depending on the interpretations and evaluation of existing information. Because this problem is unavoidable, such interpretations must be based on sound and objective information sources.

One of the major objectives in the area of large-scale modeling of systems is the construction of a causal model capable of handling the interaction among the different components of the system it represents. A causal model is based on an a priori hypothesis of system behavior as well as the interaction of the various system characteristics. Such an interaction occurs in accordance with functional relationships that define the behavior of the system and its responses in terms of physical transfer functions.

This paper discusses the development of a set of causal models for the pavement analysis and design system (PADS). In this context, the design process is viewed as an evolution of analysis in which alternatives are continually synthesized and evaluated to determine the optimal design. The operational policies encountered in handling and maintaining the system are considered as a part of this design methodology. The overall model and its subcomponents, the structural, maintenance, and cost models, are described in detail elsewhere (1) and are reviewed very briefly below.

OVERALL MODEL

PADS consists of three subsets of models: structural model, serviceability-maintenance model, and cost model. When integrated, these models form the basis for selecting and evaluating the optimal design among various alternatives.

The macrostructure of PADS is shown in Figure 1. The structural model uses information on traffic, environment, system geometry, and material properties to yield the specified damage indicators. These are the rut depth, slope variance, and extent of cracking, and they are depicted by their statistical characteristics.

The serviceability-maintenance model uses this information and reduces it to the present serviceability index (PSI) derived from the AASHO Road Test analysis. This model also accounts for the uncertainties and variabilities. The serviceability and reliability in this model are also functions of the degree of applied maintenance.

This information is then relayed into the cost model as is other information on unit costs. The cost model provides a cost estimate for the chosen construction-maintenance strategy, which provides the basis for an optimization of the design.

Structural Model

In the structural model, the pavement is represented by three layers in which the upper two layers have finite depths and the third layer has infinite depth. Each layer may have elastic or viscoelastic properties. The materials in each layer are assumed to be isotropic and locally homogeneous but have statistical variations in space. This scatter results from the mixing, placing, handling, and testing activities, which generate spatial variability in the materials properties. The system is subjected to circular loads of varying intensity and duration. The time intervals between successive load applications are also variable to simulate the traffic conditions on a pavement. The load patterns are also random in space to simulate the channelization of traffic. Environmental changes, i.e., the temperature regimes, are chosen to represent the prevailing regional climatic conditions under which the system is studied. (The effects of moisture and its changes can be incorporated in a similar manner.) These regimes are represented by a set of temperatures that can vary daily, monthly, or yearly as desired in the particular analysis.

Because of the uncertainties and variabilities associated with the operations of a pavement, the inputs and consequently the outputs are described in terms of probabilistic distributions instead of single valued estimates.

A block diagram of the structural model is shown in Figure 2. The model is subdivided into primary and ultimate stages. In the primary stage, the response of the layered system to a static load applied at the surface is obtained by using the layered system theory (2) and closed-form analytic solutions to account for the variabilities in material properties. This stage provides statistical estimates of stresses, strains, and deflections at any point within the pavement structure for a unit load and isothermal conditions. Such system responses are obtained for different temperature regimes. These responses are combined and used as inputs to the ultimate stage, which uses stresses, strains, and deflections to obtain the components of physical damage. The damage components considered are rut depth, slope variance, and extent of cracking, which are used by AASHO to describe the serviceability of the pavement. Probabilistic closed-form solutions are used in this stage of the model.

Input Variables

The inputs to the structural model are system geometry, material properties, load characteristics, and temperature history. System geometry is expressed in terms of the heights of the first and second layers. The material properties assumed to be pertinent here are the constitutive equations and the limiting equations. The constitutive equation for each layer is given as a creep or elastic compliance, and the limiting equations are given by fatigue curves (strains versus number of cycles to failure). Poisson's ratio is set equal to one-half. The effect of its variation was found to be negligible. The creep or elastic compliances are obtained from triaxial tests and are statistically distributed. Through use of the least squares technique, the creep compliances are fitted to an exponential (Dirichlet) series of the form

$$D(t) = \eta \sum_{i=1}^{N} \overline{G}_i \exp(-t\delta_i) \tag{1}$$

where

$D(t)$ = creep compliance at time t,
δ_i = exponents of the series (generally chosen to be one order of magnitude apart from each other except for $\delta_{N=0}$),
$\overline{G}_i$ = coefficients of the Dirichlet series for the mean creep compliance,
N = number of terms in the series (generally equal to the number of decades of time covered by the experimental data), and
η = random variable with a mean of 1 and a coefficient of variation determined by the scatter of the creep functions.

For the elastic case, all $\overline{G}_i$ equal zero except $\overline{G}_N$. In the general case the instantaneous compliance is represented by $\sum_{i=1}^{N} \overline{G}_i$, and the compliance at very large times is given by $\overline{G}_N$.

In addition to the creep functions, mapping parameters are required to account for the effects of environmental variables such as temperature. When the temperature dependence is accounted for, the creep compliance is given by the following formula:

$$D(t, T) = \alpha_T + \beta_T \, \eta \sum_{i=1}^{N} \overline{G}_i \exp(-\delta_i t/a_T) \tag{2}$$

In equation 2, α_T represents a vertical shift on an arithmetic scale, β_T represents a vertical shift on a logarithmic scale, and a_T represents a horizontal shift on a logarithmic scale of time. In many cases of thermorheologically simple materials $\alpha_T = 0$. β_T is a function of temperature and density but does not vary appreciably from a value of 1, and a_T is referred to as the shift factor and is given for different temperatures. These parameters have to be determined for each type of material. Further theoretical background on the mapping procedures is given elsewhere (1).

To account for plastic deformations other than those due to rate sensitivity, equation 3 is used. These plastic deformations are considered to be principally due to differences in material response to loading and unloading cycles. Thus it is assumed that the unloading function is a certain proportion of the loading function.

$$D_{unloading}(t, N) = D_{loading}(t, N) - D_{loading}(\infty, 1)\,\mu N^{-\alpha} \tag{3}$$

where N is the number of previous loadings.

Therefore, for a unit load applied at time zero and kept for a duration Δt and then removed, the accumulated deformation at time t is

$$\epsilon_{\text{accumulated}}(t) = [D(t, 1) - D(t - \Delta t, 1)] + D(\infty, 1)\mu \qquad (4)$$

The first term in equation 4 represents the usual linear viscoelastic accumulation, and the second term represents an additional plastic deformation. The exponential factor in N is introduced to account for the decrease in the accumulation rate of plastic deformation as the degree of compaction increases. For a sequence of N loads applied at time t_n and kept for durations of Δt_n, the accumulated response is

$$\epsilon_a(t) \sum_{n=1}^{N} [D(t - t_n, n) - D(t - t_n - \Delta t_n, n)] + \sum_{n=1}^{N} D(\infty, 1)\mu n^{-\alpha} \qquad (5)$$

More details are given on the nonlinear rebound function in the literature (1).

Fatigue curves are represented by

$$N_f = K_1 (1/\Delta\epsilon)^{K_2} \qquad (6)$$

where

N_f = number of cycles to failure,
$\Delta\epsilon$ = tensile strain amplitude, and
K_1 and K_2 = coefficients related to materials characteristics.

These coefficients are generally sensitive to temperature and are also statistical in nature.

In the present analysis the following expressions were used for the mean values of these coefficients:

$$K_1 = 10^{|-10 - 0.15(70 - T)|}$$

$$K_2 = 4 + 0.04(70 - T)$$

where T is the temperature in deg. The dependency of K_1 and K_2 on temperature will be determined from further experimental data.

The coefficients K_1 and K_2 may be statistically correlated. The coefficient of correlation varies between -1 and +1. This coefficient of correlation has an important effect on the analysis. If this coefficient is -1, an increase of K_1 corresponds to a decrease of K_2; if the coefficient is zero, K_1 and K_2 are statistically independent of each other. These coefficients are given by their means, variances, and coefficient of correlation. The variances and coefficient of correlation determine whether the experimental scatter is best represented by fatigue curves rotated in a given direction or translated with respect to each other. The present analysis assumed different values for the coefficient of correlation to examine its influence.

Other coefficients of correlation that are important but not included in the computer program relate the strain amplitude $\Delta\epsilon$ to the K_1 and K_2. These coefficients of correlation are important because there is certainly a relation between the constitutive equation and the fatigue properties. For instance, a specimen with a higher-than-average modulus probably has a lower-than-average fatigue curve, even though the strains that it will experience will be lower than average (for the same loads).

The spatial coefficient of correlation completes the set of material properties. This coefficient is a measure of the statistical correlation of two points at a given distance from each other. This coefficient ρ can be represented by

$$\rho = A + B \exp(-X^2/C^2) \tag{7}$$

where X represents the distance between the two points to be correlated.

The values of ρ fall in the range of ±1. In this case, it is unlikely (not entirely impossible) to be negative. The closer it is to a value of 1, the more homogeneous are the material properties. It should be noted that $\rho = 1$ for $X = 0$, and it approaches zero as X increases. This indicates that two neighboring locations are more likely to have similar properties than two locations that are farther apart. The shape of this curve is a function of the condition of the subgrade as well as the methods of construction. In the numerical examples, the following values were arbitrarily chosen: $B = 1$, $C = 0.12$, and $A = 0$.

The application of traffic load to a pavement system is assumed to be a process of independent random arrivals. Vehicles arrive at some point on the pavement in a random manner both in space (i.e., amplitude and velocity) and in time (of arrival). The arrival process is modeled as a Poisson process with a mean rate of arrival λ. The probability of having any number of arrivals n at time t may be defined as

$$P_n(t) = \frac{\exp(-\lambda t)(\lambda t)^n}{n!} \tag{8}$$

Assumptions of stationarity, nonmultiplicity, and independence must be satisfied for the underlying physical mechanism generating the arrivals to be characterized as a Poisson process. In this context, stationarity implies that the probability of a vehicle arrival in a short interval of time t to $t + \Delta t$ is approximately $\lambda \Delta t$, for any t in the ensemble.

Nonmultiplicity implies that the probability of two or more vehicle arrivals in a short interval is negligible compared to $\lambda \Delta t$. Physical limitations of vehicle length passing in one highway lane support this assumption; it is not possible for two cars to pass the same point in a lane at the same time.

Finally, independence requires that the number of arrivals in any interval of time be independent of the number in any other nonoverlapping interval of time. In a Poisson process, the time between arrivals is exponentially distributed. This property is used to generate a random number of arrivals within any time interval t.

The amplitudes of the loads in this process are also statistically distributed in space. Traffic studies (3) have shown that a lognormal distribution is suitable to represent the scatter in load magnitude. Means and variances of load amplitudes are used to represent this scatter.

The load duration, as function of its velocity on the highway, is also a random variable. On a typical highway, for example, speeds may vary from 40 to 70 mph (64 to 112 km/h); accordingly, the load duration was assumed to have a statistical scatter represented by its means and variances from distributions obtained through traffic studies.

Figure 3 shows the statistical characteristics of typical load inputs to the model. The required inputs for the loads are as follows:

1. Rate of the Poisson process λ, i.e., rate of load applications per day, month, or year;
2. Proportion of channelized traffic, i.e., the number of considered channels (2 to 10) and the fraction of traffic going into a central path (the remainder of the traffic is equally distributed over the other channels);
3. Duration of the loads in seconds, which is related to the velocity of the vehicle and which can be approximated by the time taken to travel a distance equal to three times the diameter of the loaded area (coefficient of variation of this duration is also

given to account for the variations in velocities);

4. Radius of the loads in inches (mm);
5. Intensity of the loads or tire pressure in psi (kPa); and
6. Load amplitude (optional), which is a linear multiplier of the load's intensity, given by a mean and a standard deviation (accounts for the load spectrum).

The temperature is given by its mean and variance for each basic period, which is usually taken to be a month. Regional weather trends may be established from weather bureau data, and the period over which the temperature has certain statistical properties may be extended or shortened according to local climatic conditions.

Output Variables

The outputs include the statistical estimates of the AASHO damage indicators determined at different times.

1. Rut depth is considered to be primarily due to the channelization of traffic, which causes a differential deformation in the transverse direction. Therefore, certain assumptions must be made about the probability of a certain portion of the traffic flow running in a certain channel. Rut depth is given as a differential settlement between the most traveled channel and its surroundings.
2. Slope variance is an indication of the state of the pavement in the longitudinal direction. It is a measure of pavement roughness and is caused mainly by the variations in the properties of the construction materials. The spatial variations of the material properties may be represented by the degree of correlation between the properties of points separated by a given spacing. When this correlation coefficient is close to 1, the system will be more homogeneous and the pavement will be less likely to become rough. Obviously, the coefficient of correlation will be a function of the spacing. For points that are separated by 1 ft (0.3 m) the coefficient will approach 1, and for points separated by 1 mile (1.6 km) this coefficient will tend to be 0. Points that are far apart are more likely to have been constructed at different times from different materials, and the subgrade is more likely to be different.
3. Cracking is believed to be caused by a fatigue mechanism. Miner's linear law is used to account for the crack accumulation in the top layer. The strains at the first interface are used to determine the fatigue process. There is, however, evidence that some weakening of the base and subgrade under repeated loading may be one of the principal parameters influencing the fatigue behavior of the surface layer. Cracking is given in square yards/1,000 square yards (square meters/1000 square meters).

Operation of the Structural Model

In the operation of the structural model, material creep data are fitted by the curve fitting block so that, for each material type, a creep compliance as a function of time (or elastic compliance) plus mapping parameters such as temperature shift factor a_T can be obtained.

The resulting set of material properties, along with their coefficient of variation and the geometric and load characteristics, is input to the stationary load program. The stationary load program yields the primary responses of the system at the desired locations; these responses are obtained numerically versus time. The curve fitting block is then used again to obtain an exponential series representation of the primary responses.

These exponential series are then used as input to the random load block, along with mapping parameters, traffic and temperature histories, fatigue properties of the materials, and plastic deformation accumulation parameters developed in the stationary load program. A closed-form probabilistic solution for the primary permanent responses (stresses, strains, deflections) is used to predict rutting, cracking, and slope variance of the pavement. The required formulations are given elsewhere (1). This computation block yields the history of the statistical characteristics of the damage indicators.

Serviceability-Maintenance Model

The serviceability-maintenance model is subdivided into two submodels: a serviceability-reliability (S-R) submodel and a maintenance submodel. The total S-M model is shown in Figure 4.

Serviceability-Reliability Submodel

In the S-R submodel, the distress indicators obtained from the structural model are combined in a regression form suggested by AASHO to provide a subjective measure of the serviceability level of the system at any time period. This measure is referred to as the present serviceability index (PSI), which is expressed as

$$PSI = a_0 + a_1x_1 + a_2x_2 + a_3x_3$$

where x_1, x_2, and x_3 are functions of rut depth, slope variance, and cracking. This expression has been reformulated in light of the uncertainty associated with the damage characteristics in pavements such that statistical estimates of the PSI are obtained. From this, the probabilities of having any value of PSI at any time can be determined. These probabilities are referred to as the state probabilities. In this context, the probability, at any time, of being above some unacceptable value of PSI is defined as the reliability of the system at that time period. This can be viewed as a measure of a confidence level that the system is performing its design functions. The unacceptable limit of serviceability, which is subjectively defined by the user, generally defines some threshold for failure, from which the life expectancy of the system can be determined.

The inputs to this stage, which are the results of the structural model, are the means and variances of the damage indicators (rutting, slope variance, cracking) at different values of time. The outputs include the following.

1. Means and variances of the AASHO present serviceability index at different times are one set of outputs. The model uses the following expression for the serviceability:

$$PSI = a_0 + a_1 \log (1 + SV) + a_2\sqrt{CA} + a_3\, RD^2$$

where

SV = slope variance,
CA = cracked area, and
RD = rut depth.

In the case where these damage indicators are statistically independent of each other, the following formula is obtained for the expected value of the serviceability index:

$$E(PSI) = a_1 + a_2 \left[\log(1 + \overline{SV}) - \tfrac{1}{2}(1 + \overline{SV})^2\, \sigma^2_{SV}\right]$$
$$+ a_3\left(\sqrt{\overline{CA}}^{\,-3/2}\, \sigma^2_{CA}\right) + a_4\, (\sigma^2_{RD} + \overline{RD}^2)$$

The upper bars represent an expected value, and σ^2 represents a variance (1).

2. The reliability of the system at various times assumes that the serviceability index has a normal distribution and that an unacceptable level of serviceability is defined. The reliability of the system at a given time is then the probability of having the system above the failure level.

3. The expected value of the life of the system is the mean time for the system to reach the failure level, in the absence of maintenance activities. The probabilistic distributions of the life, i.e., its probability mass function and its accumulative distribution function, are given also.

4. The marginal state probability is the probability of the system being between specified levels of the serviceability index.

Maintenance Submodel

The maintenance submodel is aimed at generating various maintenance strategies over the operational life of the pavement and evaluating the consequences of these strategies on the serviceability, reliability, life, and economic attributes. In addition, a decision-making algorithm is outlined (1) to select those strategies that provide optimal costs for a given design configuration.

Because of the dynamic nature of this process, the maintenance submodel must be equipped with dynamic feedbacks that loop through the S-R submodel and the cost model. After a maintenance level is generated and defined in terms of some quantifiable items, such as the percentage of ruts to be filled or cracks to be sealed, a feedback loop provides this information to the S-R submodel to modify the current status of the system. The feedback is also transmitted to the cost model to assess the economic consequences of maintenance. The process is repeated throughout the analysis horizon and for various levels of feasible maintenance strategies to determine which strategy provides optimal cost of operation for both the pavement and the vehicles using the road.

Cost Model

The cost model, which has been developed elsewhere (4, 5), determines the total costs of construction, operation, and maintenance of highway systems. It incorporates three components: construction, roadway maintenance, and vehicle operating costs. A schematic representation of its operation is shown in Figure 5. Each component in this model provides estimates of resource consumption and yields the cost estimates of these resources by using separately defined unit prices. This model, therefore, is adaptable to any economy regardless of the relative costs of various resources.

Input variables define the project to be analyzed. Also defined as input is the structural design-maintenance strategy to be evaluated. Grade, alignment, width and depth of surfacing, and maintenance and reconstruction policy are defined; and local unit costs for labor, equipment, and materials are specified. On the basis of this information the submodels estimate the construction, maintenance, and user costs for each analysis period. The model discounts these costs to find the present value of the structural design-maintenance strategy being evaluated. The designer can then compare a number of strategies on the basis of their total predicted cost. The cost model thus provides a basis for decisions on selection and operation of optimal design systems.

RESULTS AND SENSITIVITY ANALYSIS

Illustrative examples and sensitivity analyses designed to demonstrate the ability of the models to predict response of the system and its measures of effectiveness are presented. The analysis conducted in this study involves examining the model sensitivity to changes in the controllable design factors for pavement systems. The factors considered in this study are geometrical configuration, changes in material properties,

Figure 1. Macrostructure of PADS.

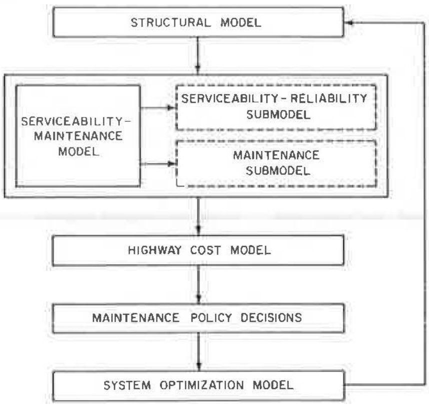

Figure 2. Structural model.

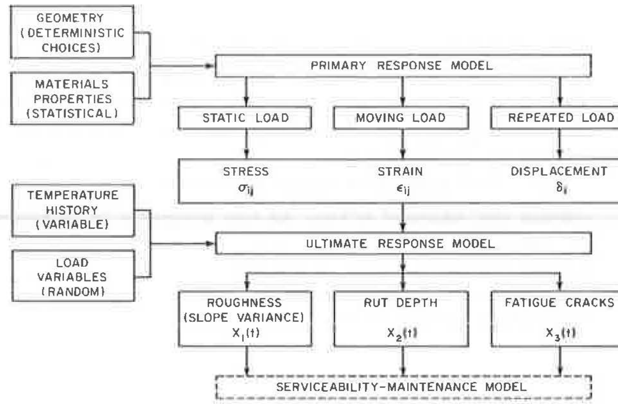

Figure 3. Distribution of load charactersitics.

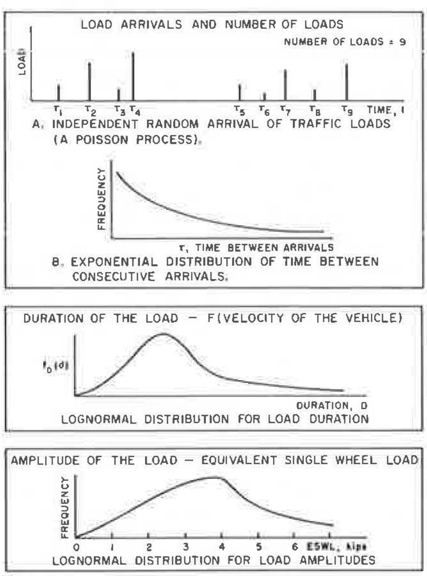

Figure 4. Serviceability-maintenance model.

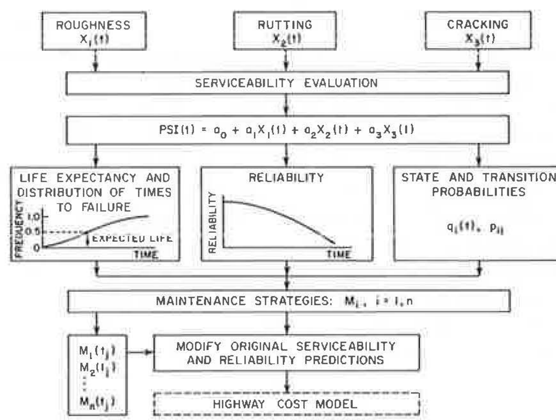

Figure 5. Operation of cost model.

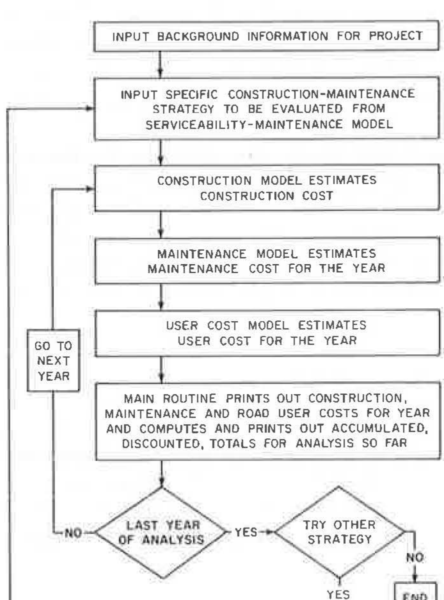

influence of quality control aspects on the damage progression within the system, and its serviceability, reliability, and life expectancy. These are essentially the parameters over which an engineer has control when designing a pavement.

To establish a common yardstick for comparison among the different systems at hand, these systems were subjected to similar load and temperature histories.

Input Descriptions

The temperature was assumed constant and equal to the reference temperature, 70 F (21 C). Hence, all the time-temperature shift factors were unity. For the fatigue curves described above, the coefficients K_1 and K_2 were assumed to have a correlation of zero, i.e., linear independence. The mean load intensity in the random loading program was 80 psi (550 kPa), with a variance of 400 psi^2 (19 000 kPa^2). The mean duration of the load is 0.05 sec with a variance of 0.0004 sec^2. The mean traffic rate was 0.01 load/sec or 864 loads/day. The coefficients of normal deflection and radial strain accumulation were taken as 0.0002 and 0.00004 respectively, and the exponents were taken as 0.6 and 0.5 respectively. The radius of the applied loading was 6.4 in. (16.2 cm). The spatial autocorrelation function assumed a coefficient of 1.0 and an exponent of 0.12. The serviceability failure level was set to 0.46 on a normalized 0-1 scale.

The usual single parameter influence on pavement behavior was not analyzed; instead, the trade-offs and interactions of several parameters were revealed by using three-dimensional plots. Accordingly, three system geometries, three sets of physical properties of the material constituents, and three levels of quality control on the system fabrication were analyzed.

The geometry of the system is expressed in terms of the thicknesses of its first and second layers; the third layer is infinitely deep. The thickness of the layers in inches (2.54 cm) is as follows:

Geometry	Layer 1	Layer 2
Thin	3	5
Medium	4	6
Thick	5	9

The physical properties of the materials can be characterized as weak, medium, and strong, depending on the creep functions of their constituent materials. These creep functions are shown in Figure 6, where the infinite time compliance of the third layer is taken as 0.001.

The levels of quality control can be characterized as poor, medium, and good. The percentage of statistical scatter in material properties is as follows:

Quality Control Level	Layer 1	Layer 2	Layer 3
Good	0	10	20
Medium	20	30	40
Poor	40	60	70

Effects on Rut Depth

Figure 7 shows the mean rut depth histories as functions of time, material quality, and system thickness (given good quality control), indicating that the mean rut depth is roughly inversely proportional to the system thickness and the material quality; there is a slight positive correlation between thickness and material quality. This agrees quite well with intuition, although the relationships may not be quite so linear. Quality

Figure 6. Creep function for (a) weak, (b) medium, and (c) strong material properties.

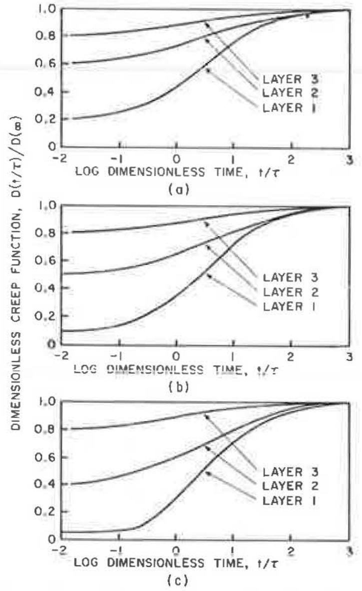

Figure 7. Rut depth as a function of material quality for (a) thin, (b) medium, and (c) thick systems.

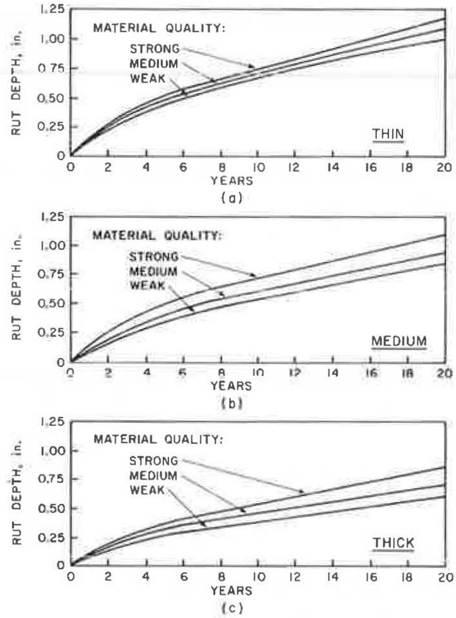

Figure 8. Slope variance as a function of quality control and time for (a) weak, (b) medium, and (c) strong material quality.

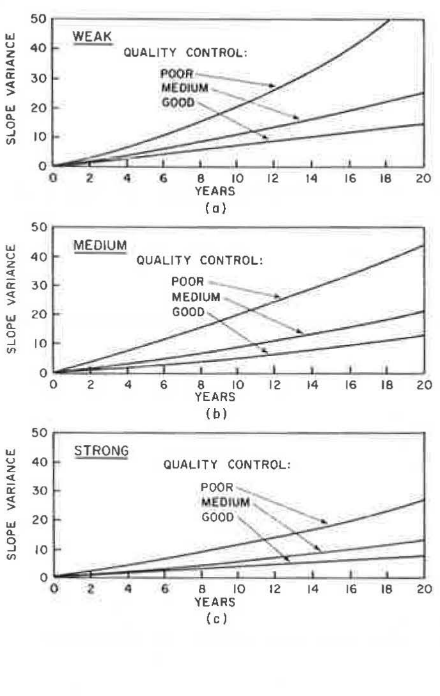

Figure 9. Cracking as a function of system thickness and time for (a) weak, (b) medium, and (c) strong material quality.

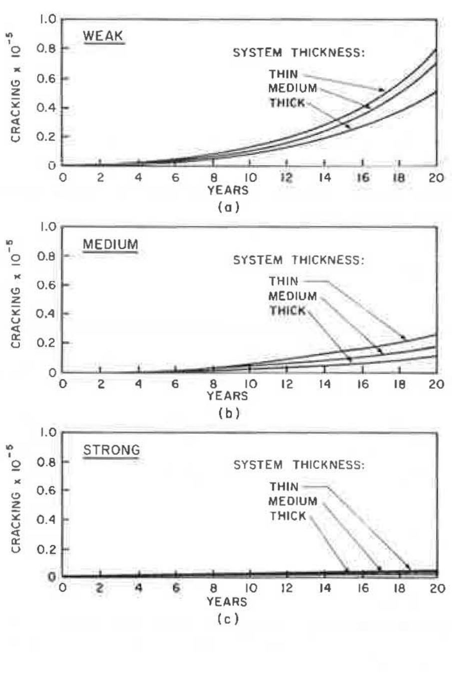

control level has a relatively insignificant effect on the mean rut depth but does influence the variance of rut depth (which is related to roughness). This is due primarily to the assumed symmetry of the creep function distributions about the mean.

Effects on Slope Variance

Figure 8 shows the mean slope variance as a function of time, material quality, and quality control (given a thin geometry). The data indicate that the mean slope variance is roughly proportional to the square of the quality control (expressed as a percentage variation) and inversely proportional to the material quality. Iterations over the system thickness reveal also that the mean slope variance is roughly inversely proportional to system thickness. The slope variance also depends on the spatial autocorrelation function, which was held constant during this analysis.

Effects on Cracking

Figure 9, which shows the mean cracking damage histories as functions of time, material quality, and quality control (given a thin geometry), indicates that the mean cracking damage is roughly inversely proportional to the system thickness and the material quality of the system (the material quality being the more dominant variable). Iterations over quality control have indicated that the mean cracking damage is relatively unaffected by quality control, but the variance of the cracking damage is highly affected, for reasons similar to those for mean rut depth.

Effects on Serviceability

Figure 10 shows the mean present serviceability histories as functions of time, material quality, and quality control (given a thin geometry) and indicates that the mean serviceability is inversely proportional to the quality control (expressed as a percentage variation) and proportional to the material quality of the system. The effects of quality control enter the serviceability index primarily through the slope variance component, but the material quality and system thickness affect all mean damage components.

Effects on Reliability

Figure 11 shows the system reliability histories as functions of time, material quality, and quality control (given a thin system geometry), indicating that the reliability is proportional to the material quality and inversely proportional to the square of the quality control (expressed as a percentage variation). Iterations over system thickness indicate that the reliability is also proportional to the square of the system thickness.

Effects on Marginal Probabilities

The marginal state probabilities as functions of time and system thickness are shown in Figure 12, which indicates that the thicker the system is the slower it deteriorates. Figure 13 shows the marginal probabilities as functions of material quality, indicating that the stronger the materials are the slower the pavement deteriorates. Figure 14 shows that quality control has a similar prolongation effect.

Effects on Life Expectancy

Figure 15 shows the life expectancy of the pavement as a function of material quality,

Figure 10. Serviceability as a function of quality control and time for (a) weak, (b) medium, and (c) strong material quality.

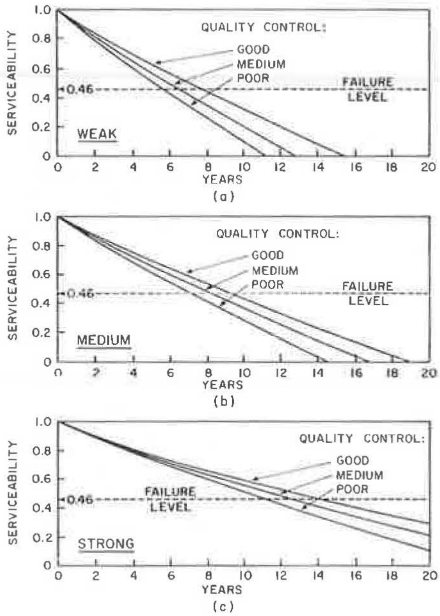

Figure 11. Reliability as a function of quality control and time for (a) weak, (b) medium, and (c) strong material quality.

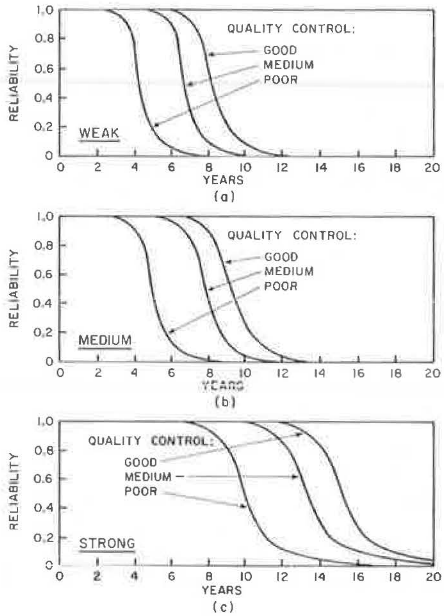

Figure 12. Marginal probabilities for (a) thin, (b) medium, and (c) thick systems.

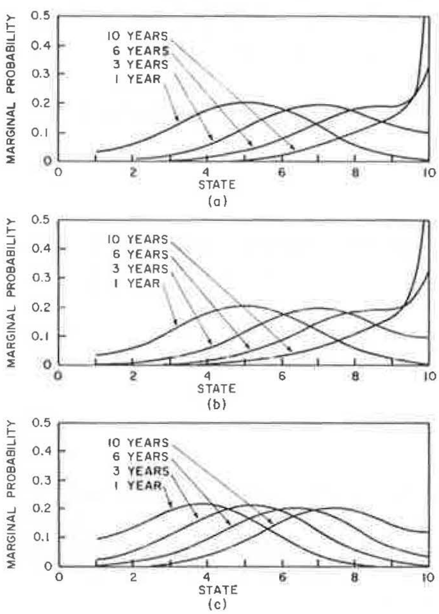

Figure 13. Marginal probabilities for (a) weak, (b) medium, and (c) strong material properties.

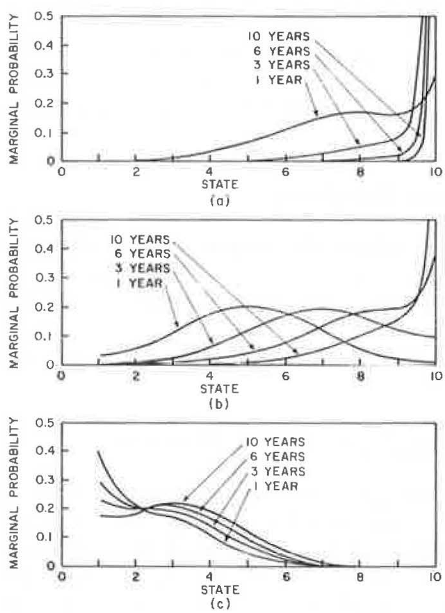

Figure 14. Marginal probabilities for (a) poor, (b) medium, and (c) good quality control levels.

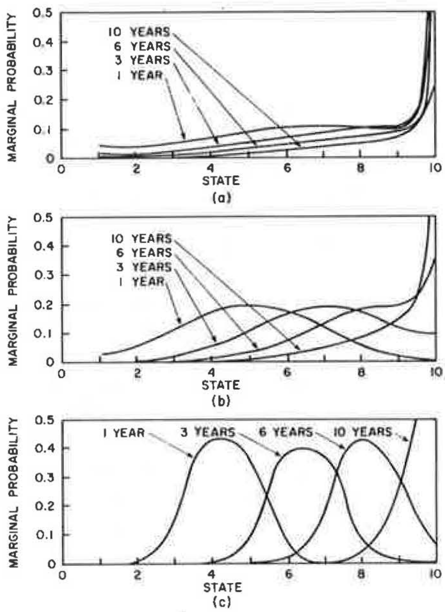

Figure 15. Life expectancy as a function of system thickness and quality control for (a) weak, (b) medium, and (c) strong material quality (given a 20-year observation period).

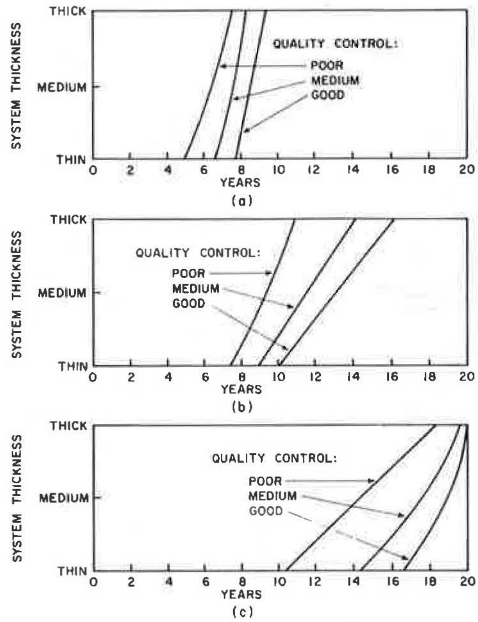

Figure 16. Serviceability as a function of system quality for the environment differing from the reference temperature (70 F, 21 C) by (a) -10, (b) 0, and (c) +10 deg.

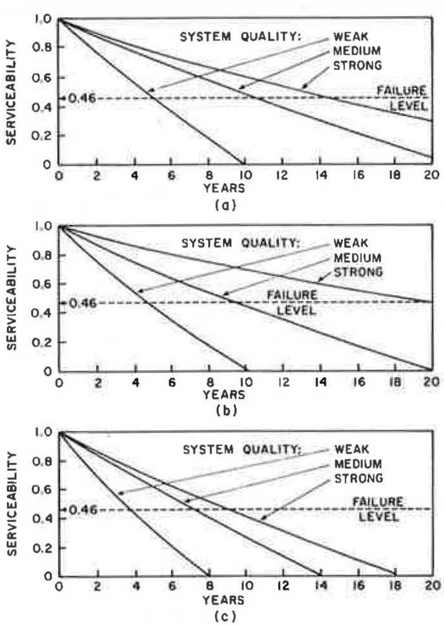

Figure 17. Reliability as a function of system quality and time for the environment differing from the reference temperature (70 F, 21 C) by (a) -10, (b) 0, and (c) +10 deg.

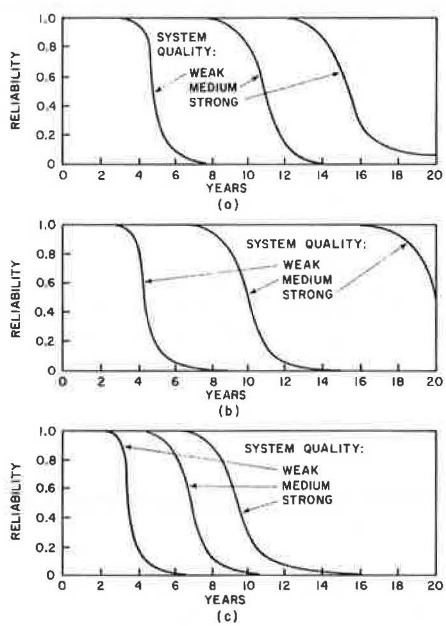

quality control, and system thickness (given a 20-year observation period). The life expectancy is roughly proportional to system thickness and the square of the material quality and is inversely proportional to quality control (expressed as a percentage variation).

Effects of System Quality and Environment on Performance

The effects of the difference between the environmental temperature and the reference temperature and of system quality on pavement performance were examined. The following three levels of system quality were selected: strong (strong material, good quality control, medium geometry); medium (medium material quality, medium quality control, medium geometry); and weak (weak material quality, poor quality control, thin geometry). The environment differed from the reference temperature by +10, 0, -10 deg F. Other variables remained as before.

Figure 16 shows the mean serviceability history as a function of time, system quality, and difference of the environment from the reference temperature. The data indicate that the mean serviceability is proportional to the system quality and is a rather complex function of temperature. This is reflected largely by the amount of creep (i.e., temperature sensitivity) of the system and by the temperature dependence of cracking damage, which appears to be minimized at the reference temperature.

Figure 17 shows reliability as a function of time, system quality, and difference from the reference temperature of the environment, indicating that the reliability is proportional to system quality and, again, a very complex function of temperature, depending on the amount of creep of the system.

Effects of System Quality and Traffic Volume on Performance

The influences of traffic volume and system quality of performance were examined. The weak, medium, and strong systems described previously were retained, and the traffic volumes were 432, 864, and 1,728 loads/day. The other inputs remained as before.

Figure 18 shows mean serviceability as a function of time, system quality, and traffic volume, indicating that the mean serviceability is more than linearly proportional to traffic volume and proportional to system quality. The degree of nonlinearity in traffic volume depends on the serviceability equation (in this case, the AASHO equation) used.

Figure 19 shows reliability as a function of time, system quality, and traffic volume. Reliability is proportional to the system quality and is a complicated function of traffic volume.

Figure 20 shows life expectancy as a function of system quality and traffic volume. There is a more than linear proportionality to system quality and an inverse proportionality to traffic volumes.

Traffic speed variations showed very little effect because of the relative constancy of the creep functions used in this time range and at the reference temperature. However, it is known from the structure of the model that the load duration influences performance measures similarly to the way environmental temperature does.

SUMMARY AND CONCLUSIONS

The basic framework and its associated models offer a very useful capability for analysis and design of highway pavements. The limited sensitivity analysis conducted so far shows some of the potentials and capabilities of the model and reveals some of the improvements necessary for full implementation of the models as a design tool.

The structural model satisfactorily accounts for the infinitesimal strains and deflections and is therefore most useful in predicting the onset of failure, although it becomes rather inaccurate as failure progresses and the system undergoes major distortions

Figure 18. Serviceability as a function of system quality and time for (a) light, (b) medium, and (c) heavy traffic volume.

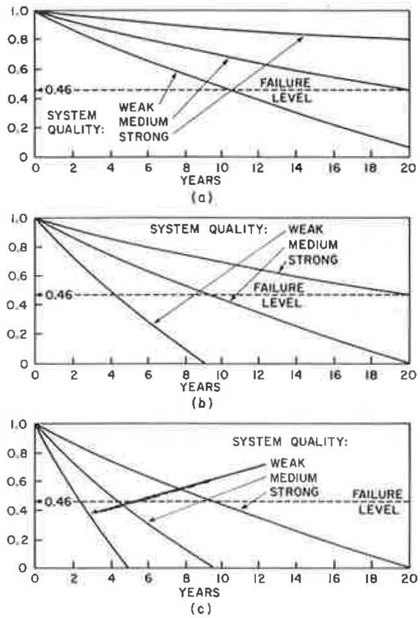

Figure 19. Reliability as a function of system quality and time for (a) light, (b) medium, and (c) heavy traffic volume.

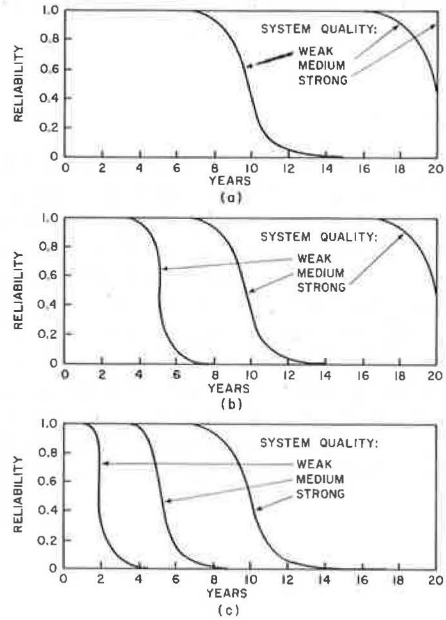

Figure 20. Life expectancy as a function of system quality and traffic volume (given medium traffic speed).

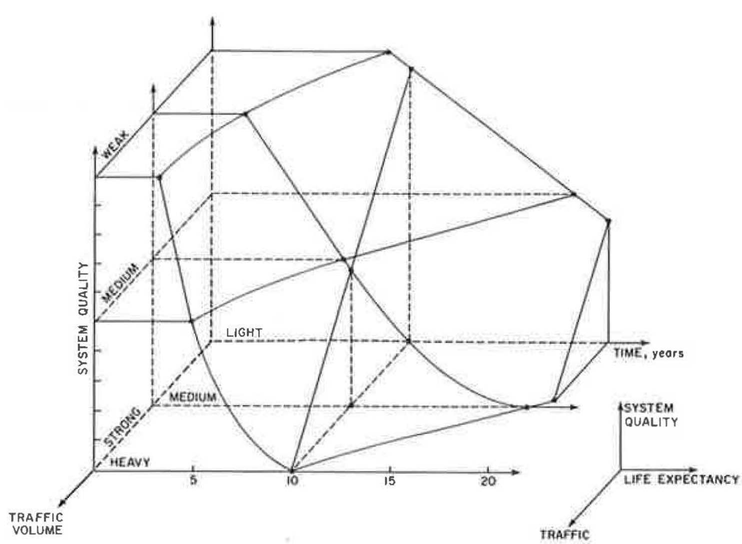

that invalidate the basic assumptions underlying the development of the models. Based on these limitations, the models may be used to compare various design alternatives. The effect of geometry, load area and intensity, random interarrival times of vehicles, statistical variations in the materials properties, and temperature histories can be accounted for by the models.

REFERENCES

1. F. Moavenzadeh, J. E. Soussou, and H. K. Findakly. Synthesis for Rational Design of Flexible Pavements. M. I. T., 1974, 3 vols.
2. J. E. Ashton and F. Moavenzadeh. Analysis of Stresses and Displacements in a Three-Layer Viscoelastic System. Second International Conference on Structural Design of Asphalt Pavements, 1967.
3. Traffic Data and Analysis on Major Highways in the State of Delaware. Delaware State Highway Department, 1962.
4. J. A. Alexander and F. Moavenzadeh. Highway Maintenance. Urban Systems Laboratory, M. I. T., Rept. TR70-38, 1970.
5. F. Moavenzadeh, J. Stafford, J. Suhrbier, and J. Alexander. Highway Design Study Phase I: The Model. International Bank for Reconstruction and Development, Economics Department Working Paper 96, 1971.

SPONSORSHIP OF THIS RECORD

GROUP 2—DESIGN AND CONSTRUCTION OF TRANSPORTATION FACILITIES
W. B. Drake, Kentucky Department of Transportation, chairman

SOIL MECHANICS SECTION
John A. Deacon, University of Kentucky, chairman

Committee on Mechanics of Earth Masses and Layered Systems
Russell A. Westmann, University of California, Los Angeles, chairman
Richard G. Ahlvin, Richard D. Barksdale, Michael I. Darter, A. Alexander Fungaroli, Charles M. Gerrard, Delon Hampton, M. E. Harr, Robert L. Kondner, Raymond J. Krizek, Fred Moavenzadeh, Keshavan Nair, Gerald P. Raymond, Robert L. Schiffman, Awtar Singh, Robert D. Stoll, Aleksandar S. Vesic, Harvey E. Wahls, William G. Weber, Jr., T. H. Wu

John W. Guinnee, Transportation Research Board staff

The organizational units and the chairmen and members are as of December 31, 1974.